

AD-A173 570

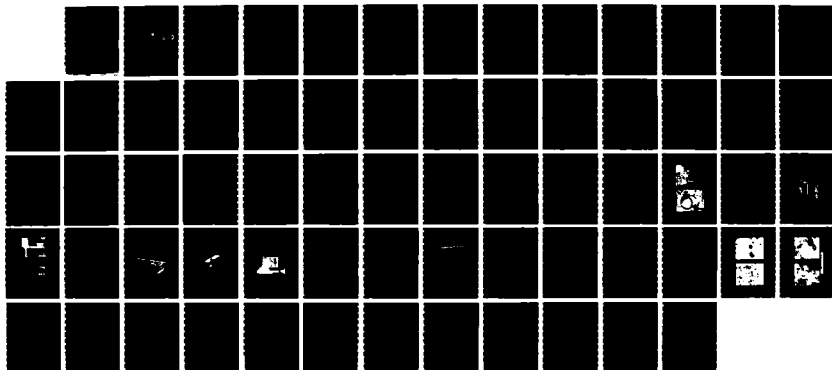
AN EXPERIMENTAL INVESTIGATION OF SOOT SIZE AND FLOW  
FIELDS IN A GAS TURBINE ENGINE AUGMENTOR TUBE(U) NAVAL  
POSTGRADUATE SCHOOL MONTEREY CA D J URICH JUN 86

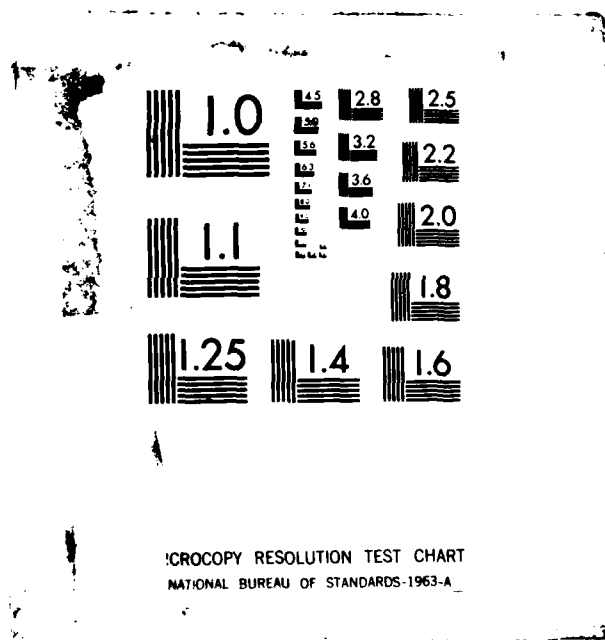
1/1

UNCLASSIFIED

F/G 21/2

NL





AD-A173 570

NAVAL POSTGRADUATE SCHOOL  
Monterey, California



DTIC  
ELECTE  
NOV 5 1986  
S B D

THESIS

AN EXPERIMENTAL INVESTIGATION OF SOOT SIZE  
AND FLOW FIELDS IN A GAS TURBINE  
ENGINE AUGMENTOR TUBE

by

Dave Jeffrey Urich

June 1986

Thesis Advisor:

David W. Netzer

Approved for public release; distribution is unlimited

NTC FILE COPY

86-11 4 064

UNCLASSIFIED

SECURITY CLASSIFICATION OF THIS PAGE

A1-A173.520

## REPORT DOCUMENTATION PAGE

1a REPORT SECURITY CLASSIFICATION UNCLASSIFIED		1b. RESTRICTIVE MARKINGS	
2a SECURITY CLASSIFICATION AUTHORITY		3 DISTRIBUTION/AVAILABILITY OF REPORT Approved for public release; distribution is unlimited	
2b DECLASSIFICATION/DOWNGRADING SCHEDULE		5 MONITORING ORGANIZATION REPORT NUMBER(S)	
4 PERFORMING ORGANIZATION REPORT NUMBER(S)		7a. NAME OF MONITORING ORGANIZATION Naval Postgraduate School	
6a. NAME OF PERFORMING ORGANIZATION Naval Postgraduate School	6b OFFICE SYMBOL (If applicable) Code 67	7b. ADDRESS (City, State, and ZIP Code) Monterey, California 93943-5000	
6c. ADDRESS (City, State, and ZIP Code) Monterey, California 93943-5000		9. PROCUREMENT INSTRUMENT IDENTIFICATION NUMBER	
8a NAME OF FUNDING/SPONSORING ORGANIZATION Naval Air Propulsion Center	8b. OFFICE SYMBOL (If applicable)	10 SOURCE OF FUNDING NUMBERS	
8c. ADDRESS (City, State, and ZIP Code) Trenton, N. J. 08628-0176		PROGRAM ELEMENT NO N6237686WR 00013	TASK NO WORK UNIT ACCESSION NO
11 TITLE (Include Security Classification) AN EXPERIMENTAL INVESTIGATION OF SOOT SIZE AND FLOW FIELDS IN A GAS TURBINE ENGINE AUGMENTOR TUBE			
12 PERSONAL AUTHOR(S) Urich, Dave J.			
13a TYPE OF REPORT Engineer's Thesis	13b TIME COVERED FROM TO	14 DATE OF REPORT (Year, Month, Day) 1986, June	15 PAGE COUNT 65
16 SUPPLEMENTARY NOTATION (see p 4)			
17 COSATI CODES		18. SUBJECT TERMS (Continue on reverse if necessary and identify by block number)	
FIELD	GROUP	SUB-GROUP	
		Soot Sizing; Velocity Flow Fields, (Theses)	
19 ABSTRACT (Continue on reverse if necessary and identify by block number) An instrumented augmentor tube was constructed and used to obtain velocity and temperature profile measurements as a function of augmentor inlet to gas generator nozzle spacing for use in Phoenix computer code validation.  Additionally, optical particle size measurement instrumentation in the form of a three wavelength transmission device and a two forward-angle scattering device using a helium-neon laser was designed, constructed and utilized for determining the effects of the augmentor flow on the change in soot size across the length.  Various smoke suppressant fuel additives were also evaluated for their effect on the soot size changes across the augmentor tube length.			
20 DISTRIBUTION/AVAILABILITY OF ABSTRACT <input checked="" type="checkbox"/> UNCLASSIFIED/UNLIMITED <input type="checkbox"/> SAME AS RPT <input type="checkbox"/> DTIC USERS		21 ABSTRACT SECURITY CLASSIFICATION Unclassified	
22a NAME OF RESPONSIBLE INDIVIDUAL Prof. David W. Netzer		22b TELEPHONE (Include Area Code) (408) 646-2980	22c OFFICE SYMBOL Code 67Nt

UNCLASSIFIED

SECURITY CLASSIFICATION OF THIS PAGE (When Data Entered)

#19 - ABSTRACT (CONTINUED)

The initial tests indicated that particle size increased significantly across the augmentor tube length.



Accession For	
NTIS ERARI	<input checked="checked" type="checkbox"/>
DTIC TAB	<input type="checkbox"/>
Unannounced	<input type="checkbox"/>
Justification	
By	
Distribution/	
Availability Codes	
Dist	Avail and/or Special
A-1	

1. N. 122-45-214-0001

UNCLASSIFIED

SECURITY CLASSIFICATION OF THIS PAGE(When Data Entered)

Approved for public release; distribution is unlimited.

An Experimental Investigation of Soot Size and Flow Fields  
in a Gas Turbine Engine Augmentor Tube

by

Dave Jeffrey Urich  
Lieutenant, United States Navy  
B. S., Pennsylvania State University, 1977

Submitted in partial fulfillment of the  
requirements for the degree of

AERONAUTICAL ENGINEER


from the

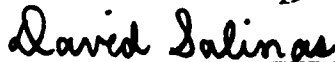
NAVAL POSTGRADUATE SCHOOL  
June 1986

Author:

  
Dave Jeffrey Urich


Approved by:

  
David W. Netzer, Thesis Advisor



D. Salinas, Second Reader

  
M. F. Platzter, Chairman,  
Department of Aeronautics

  
John N. Dyer,  
Dean of Science and Engineering

# ABSTRACT

V  
An instrumented augmentor tube was constructed and used to obtain velocity and temperature profile measurements as a function of augmentor inlet to gas generator nozzle spacing for use in Phoenix computer code validation.

Additionally, optical particle size measurement instrumentation in the form of a three wavelength transmission device and a two forward-angle scattering device using a helium-neon laser was designed, constructed and <sup>used</sup> ~~utilized~~ for determining the effects of the augmentor flow on the change in soot size across the length.

Various smoke suppressant fuel additives were also evaluated for their effect on the soot size changes across the augmentor tube length.

The initial tests indicated that particle size increased significantly across the augmentor tube length.

keywords: → (to p 1)

## TABLE OF CONTENTS

I.	INTRODUCTION -----	11
II.	EXPERIMENTAL APPARATUS -----	15
	A. GENERAL DESCRIPTION -----	15
	B. AUGMENTOR TUBE -----	16
	C. PARTICLE SIZING SYSTEMS -----	18
	1. Three Wavelength Light Transmission Apparatus -----	18
	2. Forward Scattered Light Intensity Apparatus -----	20
	3. Scanning Electron Microscope Sampling -----	21
	D. PRESSURE AND TEMPERATURE SENSING SYSTEM -----	21
	E. DATA ACQUISITION AND PROCESSING -----	22
III.	PHOENICS COMPUTER PROGRAM -----	23
	A. INTRODUCTION -----	23
	B. PHYSICAL MODEL -----	24
	C. DATA INPUT -----	25
IV.	EXPERIMENTAL PROCEDURE -----	26
V.	RESULTS AND DISCUSSION -----	29
	A. INTRODUCTION -----	29
	B. EXPERIMENTAL FLOW FIELDS -----	30
	C. PARTICLE SIZE MEASUREMENT -----	31
	1. Particle Size Effects at the Augmentor Exhaust -----	31

2. Particle Size Effects Across the Augmentor -----	33
3. Scanning Electron Microscope -----	33
VI. CONCLUSIONS AND RECOMMENDATIONS -----	35
APPENDIX A: FIGURES -----	37
APPENDIX B: TABLES -----	54
LIST OF REFERENCES -----	63
INITIAL DISTRIBUTION LIST -----	64

### LIST OF TABLES

1. TRAVERSING PROBE VELOCITY AND TEMPERATURE DATA, RUN #1 -----	54
2. X-RAKE VELOCITY AND RUN DATA, RUN #1 -----	55
3. TRAVERSING PROBE VELOCITY AND TEMPERATURE DATA, RUN #2 -----	56
4. X-RAKE VELOCITY AND RUN DATA, RUN #2 -----	57
5. TRAVERSING PROBE VELOCITY AND TEMPERATURE DATA, RUN #3 -----	58
6. X-RAKE VELOCITY AND RUN DATA, RUN #3 -----	59
7. SUMMARY OF OPTICAL DATA -----	60
8. PHYSICAL AND CHEMICAL PROPERTIES OF FUEL NAPC #7 -----	61
9. SUMMARY OF PARTICLE SIZES -----	62

# LIST OF FIGURES

1.	T-63 Combustor Installation -----	37
2.	Augmentor Tube (Schematic) -----	38
3.	Augmentor Tube (Photograph) -----	39
4.	Optical Equipment Cart -----	40
5.	Augmentor Tube Flow -----	41
6.	Traversing Kiel Probe -----	42
7.	Stationary Pitot Rake -----	43
8.	Three Wavelength Light Transmission Box -----	44
9.	Extinction Coefficient Ratio versus Particle Diameter -----	45
10.	Light Intensity Ratio versus Particle Diameter -----	46
11.	Sample Transmittance Data from Stripchart ---	47
12.	Velocity versus Radial Distance Graph S = 12 in, AR = 3.5 -----	48
13.	Velocity versus Radial Distance Graph S = 12 in, AR = 3.8 -----	49
14.	Velocity versus Radial Distance Graph S = 3 in, AR = 5.2 -----	50
15.	Particle Size versus Fuel-Air Ratio -----	51
16.	Scanning Electron Microscope Photograph of Soot, Impact Sample -----	52
17.	Scanning Electron Microscope Photograph of Soot, Filter Sample -----	53

# TABLE OF SYMBOLS AND ABBREVIATIONS

$C_m$	Mass concentration of particle
$D_{32}$	Volume-to-surface mean particle diameter ( $\mu\text{m}$ )
$g_c$	Gravitational constant--32.2 ( $\text{lbm}\cdot\text{ft}/\text{lbf}\cdot\text{s}^2$ )
$L$	Optical path length
$M$	Mach number prior to the shock wave
$m$	Index of refraction, relative between gas and particle
$P_s$	Static pressure ( $\text{lb}/\text{in}^2$ )
$P_t$	Stagnation pressure ( $\text{lb}/\text{in}^2$ )
$\bar{Q}$	Average extinction coefficients
$\bar{Q}_{1,2}$	Average extinction coefficient at wavelength $\lambda_1, \lambda_2$
$R$	Universal gas constant ( $\text{lbf}\cdot\text{ft}/\text{lbm}\cdot^\circ\text{R}$ )
$T$	Temperature ( $^\circ\text{R}$ )
$T_t$	Stagnation temperature
$T_{\lambda_1, \lambda_2, \lambda_3}$	Transmittances at wavelengths $\lambda_1, \lambda_2, \lambda_3$
$V$	Velocity ( $\text{ft}/\text{sec}$ )
$\gamma$	Ratio of specific heats $c_p/c_v$
$\lambda$	Wavelength ( $\text{nm}$ )
$\rho$	Particle density
$\sigma$	Standard deviation of the particle size distribution

### ACKNOWLEDGMENT

I would like to thank Dr. David Netzer for suffering through this project with me. He has exhibited tireless support, seemingly unlimited energy and knowledge which brought this thesis to a successful conclusion.

Thanks also to the Aeronautic Engineering staff of technicians, particularly Mr. Glen Middleton, whose rapid response in time of need and superb workmanship saved many a day's efforts.

## I. INTRODUCTION

Test cells are used to certify gas turbine engines after overhaul/rework and to provide a means for evaluation of new engines/components. In order not to affect the performance of the engine being tested, as well as to meet stringent environmental requirements, test cells must be constructed with much forethought.

Few new test cells are being constructed. Therefore, the existing test cells are being required to meet tighter constraints in both noise and pollutant emissions while engine types and size are changing. Methods for the initial design and subsequent modifications, as well as the design of pollution/noise abatement equipment, would be facilitated if accurate prediction capabilities for inlet air and exhaust flow fields were readily available. Current test cells use the jet ejector principle in augmentor tubes, to prevent engine exhaust gas recirculation and reduce the temperature as well as to suppress noise.

Temperature, pressure and velocity distributions in augmentor tubes, if known, would help determine materials required in construction, dimensions required for strength and adequacy of flow, and effects of pollution/noise control devices inserted into the flow.

The problem of meeting noise and pollution standards is not restricted to test installations, it also affects airports, as communities, with their pollution standards, grow closer together.

Reduction of engine/test cell emissions, resulting in both reduced exhaust opacity and mass concentrations, is an enviable goal. This has been one of the goals of an on-going investigation at the Naval Postgraduate School. Earlier testing employed a subscale test cell and augmentor tube (with a ramjet type dump-combustor to simulate the gas turbine combustor) to evaluate test cell geometry effects on exhaust emissions. Most recently, that apparatus was used to evaluate the effectiveness of smoke suppressant fuel additives. Limitations of the simulated gas turbine combustor resulted in the design and installation of a new combustor apparatus. This apparatus was based upon the use of a T-63 combustor.

Initial installation and testing conducted by Krug [Ref. 1] and Dubeau [Ref. 2] showed the T-63 apparatus provided an adequate test platform for the evaluation of combustor operating characteristics. Initial tests also showed that a three-wavelength light transmission technique was a viable non-intrusive method for in-combustor particle sizing in this installation.

Further refinement and installation of additional optical sizing techniques, including multiple-forward-angle

scattering intensities, was accomplished by Lohman [Ref. 3] and Bennett [Ref. 4]. They also implemented a computer-controlled data acquisition and reduction program.

Earlier experimentation on augmentor tubes conducted at the Naval Air Rework Facility, Alameda, California test cell by Mallon, Hickey and Netzer [Ref. 5] showed the viability of computer simulation of the test cell flow field as well as the types of difficulties that could occur in acquiring data for model validation in actual engine testing. The latter resulted from the severe temperature and pressure conditions to which the full scale testing subjected the instrumentation.

It is important to understand the processes that occur within the augmentor tube if effective controls of test cell exhaust stack emissions are to be implemented. A major question that needs to be answered is, what effects do engine operating conditions (exhaust temperature, soot characteristics, Mach number, etc.) and augmentor design have on the changes in soot size and soot and gaseous emission concentrations across the augmentor tube?

This investigation was directed at providing answers to some of these questions. An augmentor tube was added to the T-63 combustor apparatus. The tube was instrumented for flow field determinations (temperature, pressure and velocity), as well as for the measurement of particle size variations. Operating variables to be investigated

included changes in augmentation air ratio, combustor air inlet temperature, fuel composition and fuel additives. A further goal was to provide data for initial validation of the ability of the Phoenix Computer program to predict test cell augmentor tube performance.

## II. EXPERIMENTAL APPARATUS

### A. GENERAL DESCRIPTION

The "gas generator" for this investigation was an Allison T-63-A-5A gas turbine combustor (Fig. 1). The T-63, as installed by Dubeau and Krug [Refs. 1,2] and modified by Bennett [Ref. 4] was further modified to provide a converging, sonically choked nozzle of 1.56 inch diameter.

The augmentor tube, shown in Figures 2 and 3, was instrumented at stations 1.3 inches inside the bell mouth and 14.0 inches inside the exhaust end. Allowances for adjustment in the axial positioning of the tube and the use of different inlet geometries enabled different augmentation ratios to be set.

The optical measurement apparatus (Fig. 4), which included a three-wavelength light transmission device and a two-angle, forward scattering light intensity device, were cart-mounted and positioned immediately aft of the augmentor tube. Each of these optical devices provided a measurement of the mean soot particle diameter ( $D_{32}$ ).

In simultaneous research conducted by Jway, the T-63 exhaust mean particle size and concentration, as well as the combustor mass flow rate, were provided as the input data for the augmentor tube.

Data acquisition of the numerous pressures, temperatures and voltages from the transmission and scattering measurement devices was accomplished by a Hewlett-Packard data acquisition system which scanned the apparatus, recorded and then processed the data.

#### B. AUGMENTOR TUBE

The augmentor tube (Fig. 5), through viscous mixing of the primary jet exhaust from the T-63 with the ambient air, entrains a mass flow such that at the augmentor exhaust, the mass flow is greater than that of the primary jet. If a sufficient length of tube is provided, the velocity (and temperature) profile at the augmentor exhaust will appear relatively flat and considerably reduced in peak magnitude. It is by this means that the exhausts of gas turbine engines are conditioned before entering a test cell exhaust stack.

For determination of the mass flow through the augmentor tube, pressures and temperatures at various tube positions had to be made. Two methods were used.

The first was an electric motor driven traversing probe (Fig. 6), which yielded stagnation pressure, stagnation temperature and static pressure. The probe, which consisted of a United Sensor KT-18-C/A-12-C Kiel probe enclosed within a 0.375 inch stainless steel tube, and a static pressure probe extension, was installed 1.3 inches inside the bell mouth of the augmentor tube.

The second method of data generation was a stationary stagnation pressure (X-shaped) rake attached 14.0 inches inside the exhaust end of the augmentor tube (Figure 7).

In the bypass-air region of the augmentor tube inlet flow, and in the augmentor tube exhaust flow, the gas was assumed to be ideal and incompressible since the air flow in these regions had very low velocity ( $M \ll 1.0$ ). Thus the velocity was determined using

$$V = [2(P_t - P_s)RT/P_s]^{1/2} \quad (1)$$

Within the central core of the augmentor inlet flow, the flow was near-sonic due to underexpansion of the T-63 choked exhaust nozzle. In this region compressibility effects could not be ignored and the velocity was determined as follows:

$$V = \{ [2/(\gamma-1)] [(P_t/P_s)^{(\gamma-1)/\gamma} - 1] [\gamma RT_{gc}] \}^{1/2} \quad (2)$$

Since  $\gamma$  varies somewhat with temperature, the measured stagnation temperature was used to estimate its value for pure air. The lean overall fuel-air ratio did not warrant any corrections for gas composition change.

The local mach numbers were determined using:

$$M = \{ [2/(\gamma-1)] [(P_t/P_s)^{(\gamma-1)/\gamma} - 1] \}^{1/2} \quad (3)$$

Similarly the static temperature was determined by:

$$T = T_t / \{1 - [(\gamma - 1)/2]M^2\} \quad (4)$$

In both regions (the bypass air region and the central core region) the stagnation temperature ( $T_t$ ) was used for initial velocity and Mach number estimations ( $T_t \approx T$ ). Iteration of equations 2 (or 1), 3 and 4 converged rapidly to a velocity.

Calculation of  $\gamma$  was done by using a polynomial fit developed by Andrews and Biblarz [Ref. 6], which allows for temperature variations.

### C. PARTICLE SIZING SYSTEMS

#### 1. Three Wavelength Light Transmission Apparatus

A device similar to that used in earlier investigations (Bennett, [Ref. 4]) was constructed (Figure 8). The general theory of operation has been presented by Cashdollar [Ref. 7] and is briefly outlined below.

Light transmitted through a suspension of particles is attenuated by diffraction, refraction, reflection and absorption. For a polydispersion of small particles the volume-to-surface mean particle diameter ( $D_{32}$ ) can be readily determined. The transmission law is given by

$$T_\lambda = \exp\{-3\bar{Q}_m L / 2\rho D_{32}\} \quad (5)$$

where:

- $T_{\lambda}$  = Transmittance at wavelength
- $\bar{Q}$  = Dimensionless extinction coefficient
- $C_m$  = Mass concentration
- $L$  = Path Length
- $\rho$  = Density of individual particles
- $D_{32}$  = Volume-to-surface mean particle diameter.

For two specific wavelengths (assuming  $C_m$ ,  $\rho$ ,  $L$  and  $D_{32}$  are constant), equation (5) results in

$$\ln T_{\lambda 1} / \ln T_{\lambda 2} = \bar{Q}_1 / \bar{Q}_2 \quad (6)$$

$\bar{Q}$  is a function of the complex refractive index of the particles, the particle diameter, the wavelength of incident light and the shape of the particle size distribution function.

Various values for the index of refraction ( $m$ ) of soot have been presented [Ref. 7]. Using these values, and assuming a log-normal particle size distribution with standard deviation  $\sigma$ , plots of  $\bar{Q}_1 / \bar{Q}_2$  versus  $D_{32}$  were obtained using a computer code provided by K.C. Cashdollar.

The apparatus uses three wavelengths, which permits three extinction coefficient ratios to be calculated (Figure 9). Values of  $m$  and  $\sigma$  are varied until all three ratios yield the same  $D_{32}$  from the measured transmittances.

Narrow pass filters of wavelengths 450, 694.3 and 1000 nm were used to provide a wavelength spread similar to those used by Cashdollar [Ref. 7].

This approach has proven acceptable for determination of  $D_{32}$  in previous studies [Refs. 6,7]. However, other non-intrusive techniques can also be used. One such technique is discussed below.

## 2. Forward Scattering Light Intensity Apparatus

Powell et al. [Ref. 9], using the measurement of scattered laser light at two forward angles, demonstrated the ability to determine  $D_{32}$  for soot without a prior knowledge of the particle index of refraction. This method is based upon ratioing the intensities in the forward Fraunhofer lobe, assuming an upper-limit distribution function for the particles [Ref. 9]. If both techniques provide nearly the same  $D_{32}$ , then confidence can be expressed in the test results for both particle size and concentration.

A graph of light intensity ratio versus mean particle diameter for 20 and 40 degree scattering angles and 632.8 nm light wavelength (Figure 10, [Ref. 4]) was used for mean particle diameter determination. The light intensity ratio was measured by two photodiodes. The photodiodes had to be calibrated for differences in sensitivity. In addition, since the scattering volume

varies inversely with the sin of the scattering angle the ratio  $I_{40} \sin 40^\circ / I_{20} \sin 20^\circ$  was used to enter Figure 10.

### 3. Scanning Electron Microscope Sampling

For a final validation of the two optical techniques previously described, scanning electron microscope pedestals were inserted into the exhaust flow as well as through .2 micron filters for sample collection. Sample photographs are presented in Figures 16-17.

#### D. PRESSURE AND TEMPERATURE SENSING SYSTEM

The stagnation pressures 1.3 inches inside the bell mouth were measured with a modified United Sensor KT-18-C/A-12-C Kiel probe (Figure 6). The static pressure was measured with a standard static probe. The pressures were repeatedly scanned and recorded while the probe traversed the augmentor tube.

The probe additionally provided the total temperature measurement.

The stagnation pressure rake used at the aft end of the augmentor tube had 20 probes, 0.75 inch apart. Each probe was attached to a model J Scanivalve. Static pressure ports in the augmentor tube wall were manifolded together and also attached to the Scanivalve. A chromel-alumel thermocouple was placed in the flow aft of the rake, for temperature data. Since velocities were quite low in this region the static and stagnation temperatures were essentially the same.

#### E. DATA ACQUISITION AND PROCESSING

A Hewlett Packard data acquisition system including a HP 3456A digital voltmeter, a HP 3497A controller and a HP 9836S computer were programmed for the calibration, initial set-up of gaseous flows, primary data acquisition and processing of each data run. Back-up and cross-checking was accomplished with strip chart recordings of crucial data.

### III. PHOENICS COMPUTER PROGRAM

#### A. INTRODUCTION

The Phoenix (Parabolic, Hyperbolic or Elliptic Numerical Integration Code Series) program is a Fortran computercode for analysis of fluid flow, heat transfer and other related phenomena. The code is the work of D.B. Spaulding and Associates of Imperial College, London, England, using state-of-the-art numerical solution algorithms and turbulence models. Phoenix consists of two distinct programs, the first program, called Earth, contains the main software for modeling the laws of physics applied to elements of space and time. This portion is basically not accessible to the user, but is activated by the second portion called Satellite. Satellite accepts the user description of the problem, converts the description into data input for Earth and then activates Earth into an analysis mode.

The code, once installed, is user friendly and features graphical output, restart capability and a monitoring option. One, two and three-dimensional, steady or unsteady-state problems can be solved using Phoenix.

Conservation laws are discretized in terms of dependent variables and coefficients. The coefficients are obtained from an integration over a control volume of the field

operators, using the subdomain method from the general method of weighted residuals. The discretized equations, in general, are nonlinear and have to be solved repeatedly with updated coefficients. Convergence to a solution may be improved by using the under-relaxation option available.

#### B. PHYSICAL MODEL

The augmentor tube was modeled as an axisymmetric body as displayed in Figure 5. Initially, a step-velocity profile was used as input to the code. The combustor exhaust jet was taken to be Mach = 1.0 at 1030°F (1892 ft/sec). The augmentor bypass region was assumed to provide an augmentation ratio of 10 with a uniform velocity profile of 67.2 ft/sec at 68°F. The initial conditions at the exhaust of the augmentor tube were input as 68°F at 14.7 psi.

In attempts to more accurately model the expected inlet velocity profile, successive refinements of the input data were tried. This was accomplished by increasing the number of steps at varying velocities. Actual model validation will be conducted using the flow field as collected by the traversing probe as displayed in the Data Input section that follows (and Figures 12-13). Initial use of the code treated the flow as incompressible. This cannot be expected to yield accurate results for sonic or supersonic engine exhaust velocities, but was done to obtain initial familiarity with the code.

### C. DATA INPUT

For validation of the Phoenix code for use in augmentor tube design, the velocity and temperature profiles at the augmentor inlet were required. Instrumentation in the form of the traversing Kiel probe provided pressure and temperature profiles which were manipulated as described previously to yield the desired velocity and temperature profiles.

Tables 1 through 6 are a compilation of the data obtained in three separate runs. They included a wide spread in operating conditions, such as spacing of augmentor-to-nozzle and gas temperature, to provide a broad range of data for model validation. These tables constitute the input required for the Phoenix code.

#### IV. EXPERIMENTAL PROCEDURE

Experimentation was conducted in two phases. The first phase was to develop velocity and temperature profiles in the augmentor tube inlet and exhaust stations, permitting augmentation ratio to be determined. The second phase was the investigation, both optically and through particle collection, of the effect of augmentation on the change in particle size across the augmentor. While initial plans were to conduct the two phases simultaneously, the first phase was completed early and portions of the apparatus for its determination were removed to reduce complications and free instrumentation for other uses. Initial investigations for obtaining velocity profiles for Phoenix validation proceeded as follows.

The augmentor tube, which was mounted on wheels, was carefully positioned both vertically and horizontally in line with the exhaust from the nozzle of the T-63 combustor. Once positioned, it was fastened down to preclude its motion as a result of being in the exhaust flow of the T-63.

All transducers were turned on for a nominal 30 minute warm-up period and then calibrated prior to each data run. Various T-63 nozzle-to-augmentor tube inlet spacings were tried to achieve a velocity profile typical for a turbojet

engine exhaust stream. Both cold blow-down air runs and hot runs with the T-63 ignited were conducted.

Recording instrumentation and the computer acquisition systems were turned on and the desired air flow was set. Once the area was cleared of personnel the T-63 was ignited and the apparatus was permitted to achieve steady-state run conditions. Computer-controlled acquisition of data started with a scan of the X-pitot rake pressures and temperature. This was followed by a pass of the traversing Kiel probe across the augmentor tube inlet. Optical data was then collected in the T-63 and the augmentor tube exhaust. This procedure was accomplished twice for each run sequence.

Following completion of the first phase of tests, the procedure was as follows. The cart with augmentor optical particle measurement instrumentation was positioned immediately aft of the augmentor tube. Light and laser alignment were checked and 0% and 100% transmittance values were recorded by the computer and strip charts following a 30 minute warm-up period. The test run was initiated with a scan of temperature and pressures and followed with a scan of all optical instrumentation, once steady-state run conditions were achieved. Fuel additive pumps were turned on and the previous sequence was repeated. The fuel flow was stopped and blow-down air was used to cool down the apparatus. Post fire 0% and 100% readings were then

recorded. Figure 11 shows a typical stripchart of one voltage output from the three wavelength device.

## V. RESULTS AND DISCUSSION

### A. INTRODUCTION

Based on earlier results with the subscale test cell [Ref. 6], the  $D_{32}$  at the augmentor exhaust was expected to be less than 0.3 microns. This prompted the use of the three-wavelength transmission technique. Particle diameters at the exhaust of the augmentor tube were measured to be in the range of 0.31 to 0.42 microns, which is large for the three-wavelength technique. This manifested itself as a large spread in the values of  $D_{32}$  obtained from the three transmittance ratios, a direct result of all the extinction coefficient ratios approaching unity when particles exceed 0.4 microns (see Figure 9). A small variation in the extinction coefficient ratio results in a large change in  $D_{32}$ .

Attempts at calibration using National Bureau of Standard 0.9 micron polystyrene beads also resulted in a wide spread, centered on .9 micron. Transmittances in the range of 85% provided the smallest spread in the calibration attempts.

The transmittances in the exhaust stream were high, approximately 95%, which prompted the utilization of a double pass of light through the augmentor exhaust stream, as well as the installation of a blocking plate at the

inlet of the augmentor tube to reduce the dilution of the soot. The blocking plate resulted in an augmentation ratio of 0.53 and transmittances of approximately 89%.

As a cross-check for particle size, a two-angle forward scattering device was installed. This device provided relatively consistent particle size data. This data was in good agreement with the data obtained using the three-wavelength device, when the latter did not exhibit its characteristic spread. As a result, the light scattering measurement device appeared to provide good data.

#### B. EXPERIMENTAL FLOW FIELDS

The traversing Kiel probe was originally designed for use in flows with less than sonic velocity. Initial utilization, however, showed regions of supersonic flow in the expansion of the underexpanded exhaust jet of the sonically choked T-63 nozzle. This invalidated the assumption that the static pressure would be relatively constant across the augmentor inlet. Modifications to the probe were then made, which included a static port extension (as seen in Figure 6) and strengthening of the probe support. Furthermore, in actual data runs, efforts were made to ensure that the Mach number was as low as possible to reduce measurement errors. Tables 1 through 6 are a compilation of the three runs selected for initial Phoenix validation. Plots of the same data appear in Figures 12 and 13.

Efforts to use Phoenix are underway, and have not been completed to date. Installation of Phoenix into the Naval Postgraduate School's IBM 370 series in its user friendly form has not occurred during the span of this thesis. The code, as available, requires tedious submission and debugging processes. These problems are the object of another research effort, and will continue.

#### C. PARTICLE SIZE MEASUREMENT

Table 7 is provided as a summary of all pertinent runs and shows the transmittances for the three wavelengths, particle diameter from each extinction ratio, the scattered light intensity ratio and the corresponding particle diameter. These runs were all conducted with the T-63 exhaust nozzle flush with the blocking plate. The fuel used was Naval Air Propulsion Center-provided NAPC #7. Fuel properties are presented in Table 8. Additives tested were 12% Cerium Hex-Cem, Ferrocene Solution and USLAD-2055. Table 9 is provided for comparison of fuel-air ratio, temperature and augmentation effects on particle size.

##### 1. Particle Size Effects at the Augmentor Exhaust

In these initial tests there were insufficient temperature measurements taken throughout a given run to accurately determine the effect of augmentor exhaust temperature on particle size. However, the augmentor exhaust temperature followed the engine exhaust temperature

(fixed augmentation air dilution) which was recorded continuously throughout the run.

With one exception (Run 8,8a), the particle size appeared to increase with fuel-air ratio (Figure 15). This was evident in Runs 9, 10, 11, 12 and 16. Run 8 and 8a exhibited a soot blow-out which resulted in a wide range in measured transmittances (evidenced on the strip chart data and visually).

Although the accuracy of the particle size measurements may result in questionable conclusions, there did seem to appear to be a small, but consistent, increase in augmentor exhaust particle size with increasing temperature. This was in contrast to a slight decrease in  $D_{32}$  at the combustor exit with increasing temperature.

All additives exhibited the same approximate effect at the augmentor tube exhaust. For each run in which an additive was used (Runs 8, 8a; 9, 9a; 10, 10a; 11, 11a; 12, 12a; 13, 13a; 16, 16a) the particle size increased approximately 0.02 microns. While the additive effect on  $D_{32}$  was small, it appeared as a consistent slight increase. Generally, transmittance increased with the use of additives.

The soot mass concentration should not change appreciably across the augmentor tube since temperatures are quite low. However soot deposits on the tube walls can remove some soot from the flow. There was no consistent

trend in the calculated change in  $C_m$  when the additives were used.

Only one hot combustor air inlet run was made (Runs 13, 13a), resulting in the expected increase in engine exhaust temperature at the same fuel-air ratio (compare to Runs 16, 16a). It appears that  $D_{32}$  decreased significantly at the augmentor tube exhaust as the air temperature in the augmentor was raised. There was a similar effect noted in the T-63, itself, by Jway.

## 2. Particle Size Effects Across the Augmentor

From Runs 8a, 9, 9a, 10, 10a and 13, it is evident that the mean particle diameter nearly doubled from the T-63 exhaust to the augmentor tube exhaust. This could be caused by several effects; agglomeration of particles or the walls shedding of previously impacted soot (all test runs had sooted walls in the augmentor tube).

## 3. Scanning Electron Microscope

Figures 16a and 16b show the typical impact collected test sample. A large variation in sizes is exhibited with the largest being approximately 1.5 microns and the smallest in the submicron range. The Hitachi 265s scanning electron microscope provides good resolution, however the carbon make-up of the particles did not lend itself to good viewing without being flashed with gold. The specimen presented in Figures 16a and b were not coated and developed a radiance or ghostlike appearance.

In Figures 17a and b the specimens were gold flashed (0.2 micron pore) filter paper on which the soot was collected through a 1/4-inch sampling tube. Again, a substantial variation in particle size from submicron to larger than 1.0 micron was observed.

$D_{32}$  is dominated by the larger particles in a distribution. Thus, the optically measured  $D_{32}$  of approximately .34-.42 microns appears to be quite realistic.

## VI. CONCLUSIONS AND RECOMMENDATIONS

The effects of augmentation air within the augmentor tube on particle size appeared two-fold. The first was that the particles appeared to approximately double in size across the augmentor, due to agglomeration or wall shedding of previously impacted soot. The second effect was an increase in the transmittance through gross dilution with secondary air. Each of these effects could be exploited for providing a reduced stack opacity in the test cell environment.

The mean particle diameter at the augmentor exhaust was also influenced by the engine operating condition. Increased combustor inlet air temperature (and the corresponding increase in engine exhaust temperature) resulted in a significant reduction in particle diameter (more so than the reduction observed at the combustor exhaust).

In regard to the apparatus in its present configuration, improvements to refine the measurements and increase confidence in the data obtained are required. Recommendations are:

1. The addition of another scattering angle device at  $10^\circ$  to provide three ratios for comparison. The correlation of three diameters determined from the ratios of  $I_{40}/I_{20}$ ,  $I_{20}/I_{10}$  and  $I_{40}/I_{10}$  would increase the level of confidence in each data run.

2. Since little data correlation was obtained using the three-wavelength method, the method should probably be discontinued.
3. A series of tests needs to be conducted in which the additive run is accomplished first in the run sequence to determine if the effect of the additives is repeatable. This is needed as all the data tabulated herein were obtained with the additive series second in the sequence.
4. Further testing with different augmentation ratios needs to be accomplished to investigate the effects on soot agglomeration.
5. Augmentor runs should be tried with cleaned walls to determine if soot shedding is promoting the large particle sizes which were measured or a bi-modal distribution in the augmentor exhaust. The latter could invalidate both of the optical sizing techniques employed.
6. The scanning electron microscope proved quite valuable in validating the optical techniques. Due to uncertainties in the collection method it cannot be said whether the large (~ 1.5 micron) particles were agglomerates from the flow or from the augmentor tube shedding. Additional work to improve the particle collection technique is needed to further validate the optical measurements.

The traversing  $P_t/T_t/p$  probe appeared to work satisfactorily. However, the aft rake design needs to be improved to withstand the high gas temperatures which exist at low augmentation ratios.

APPENDIX A

FIGURES

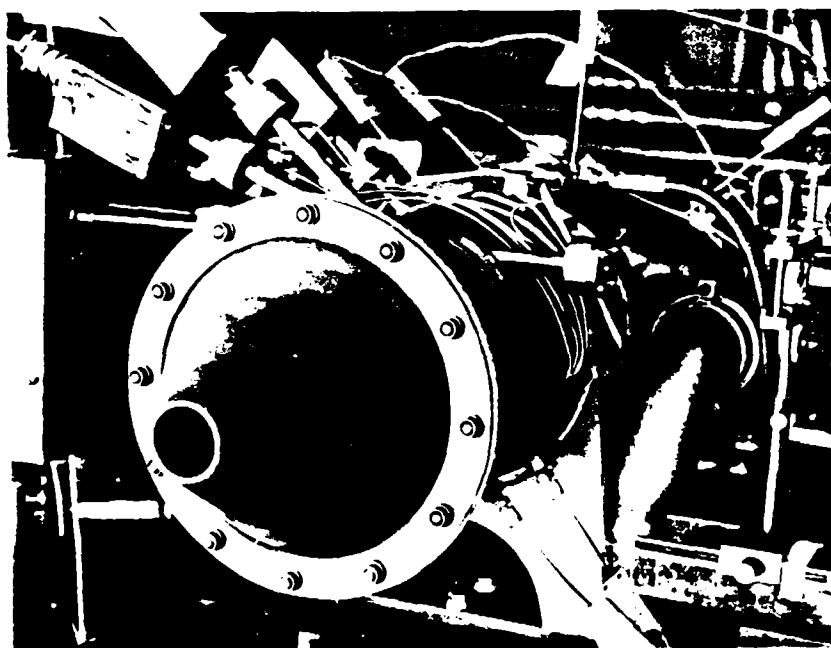
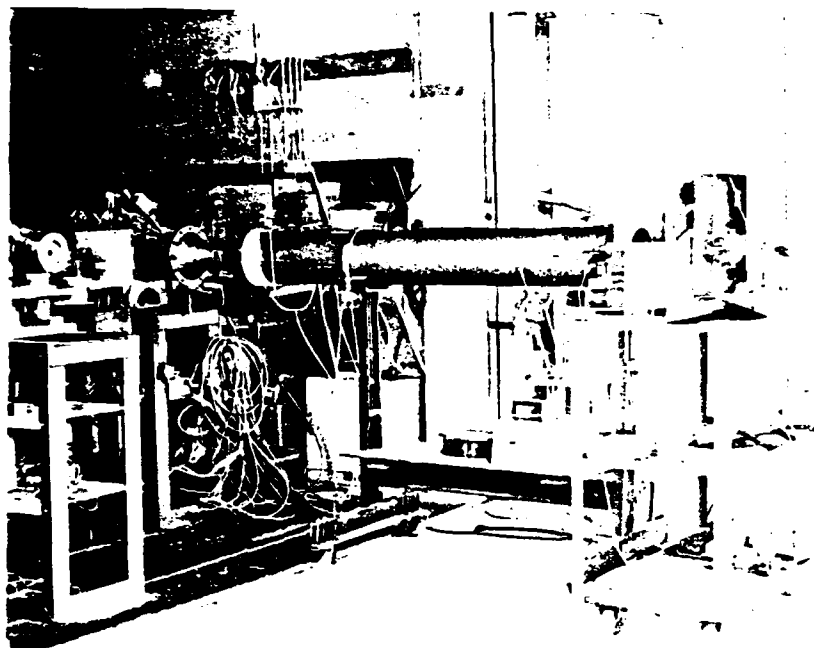


Figure 1. T-63 Combustor Installation

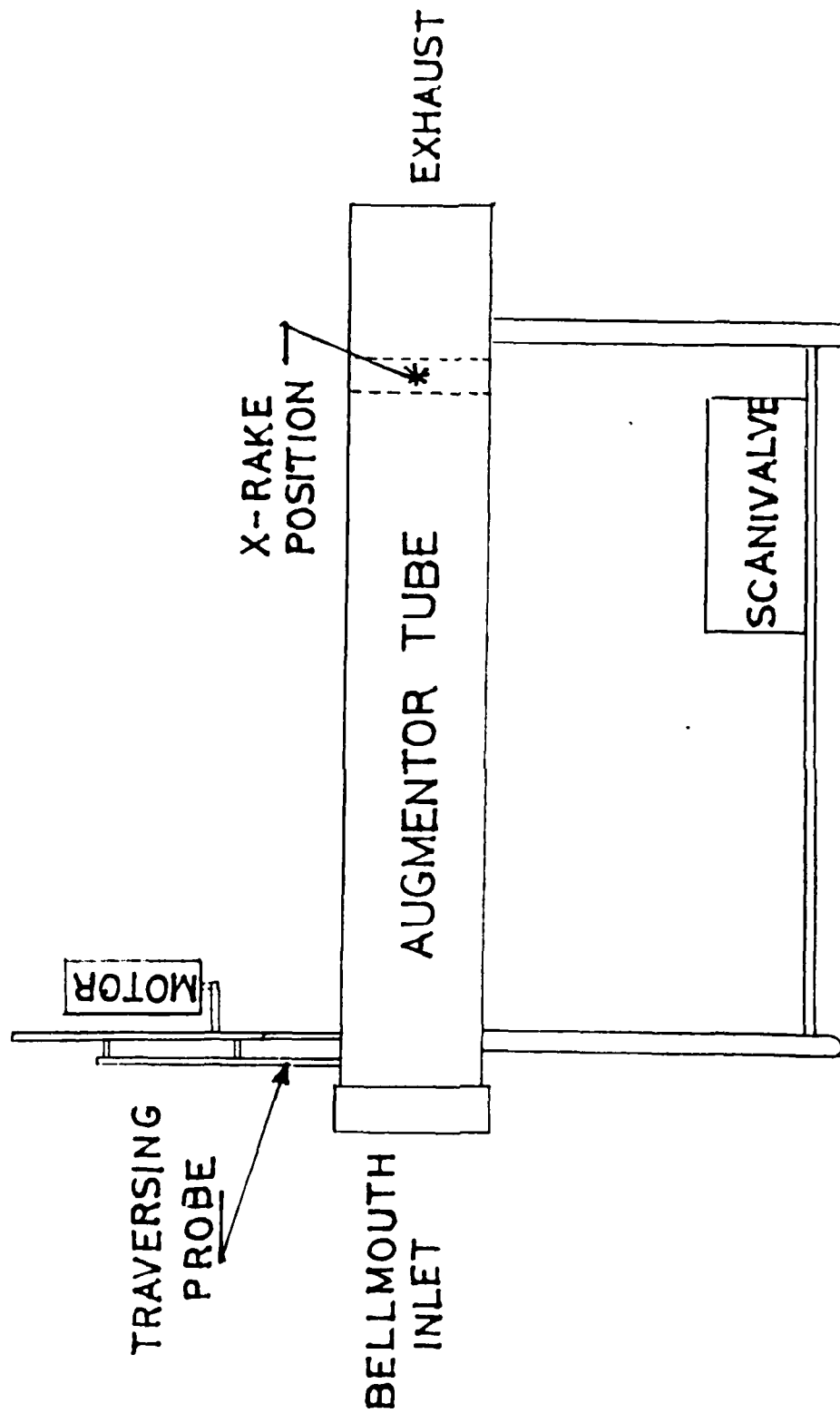


Figure 2. Augmentor Tube (Schematic)

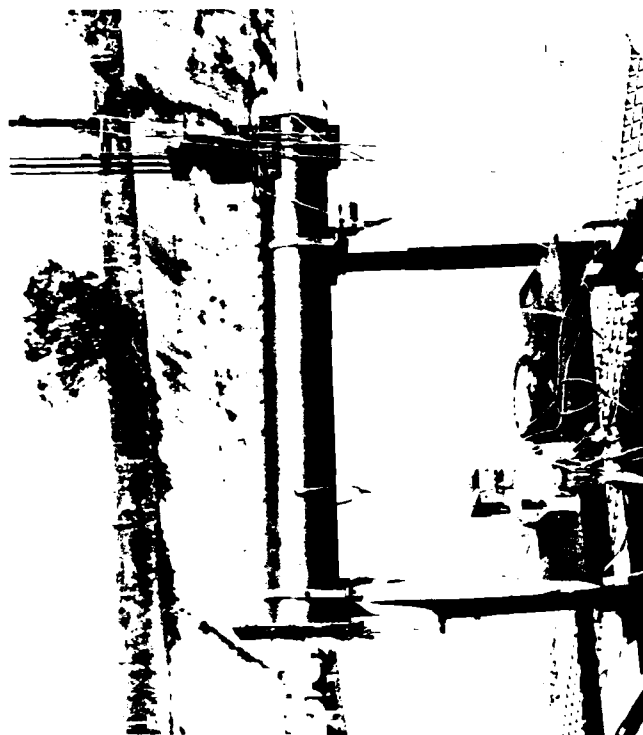


Figure 3. Augmentor Tube (Photograph)

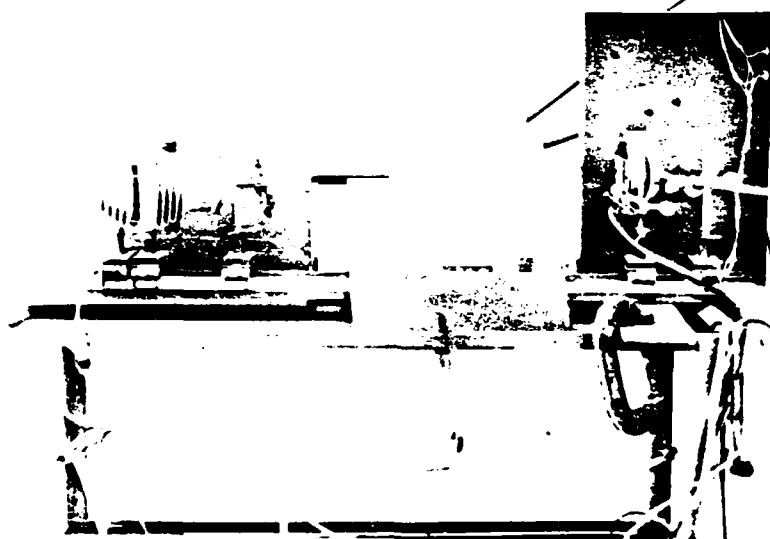
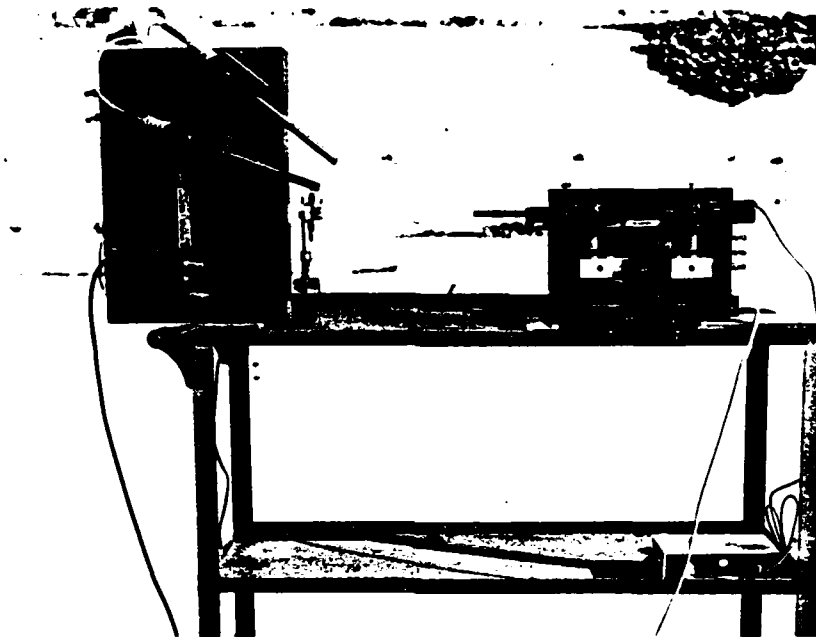


Figure 4. Optical Equipment Cart

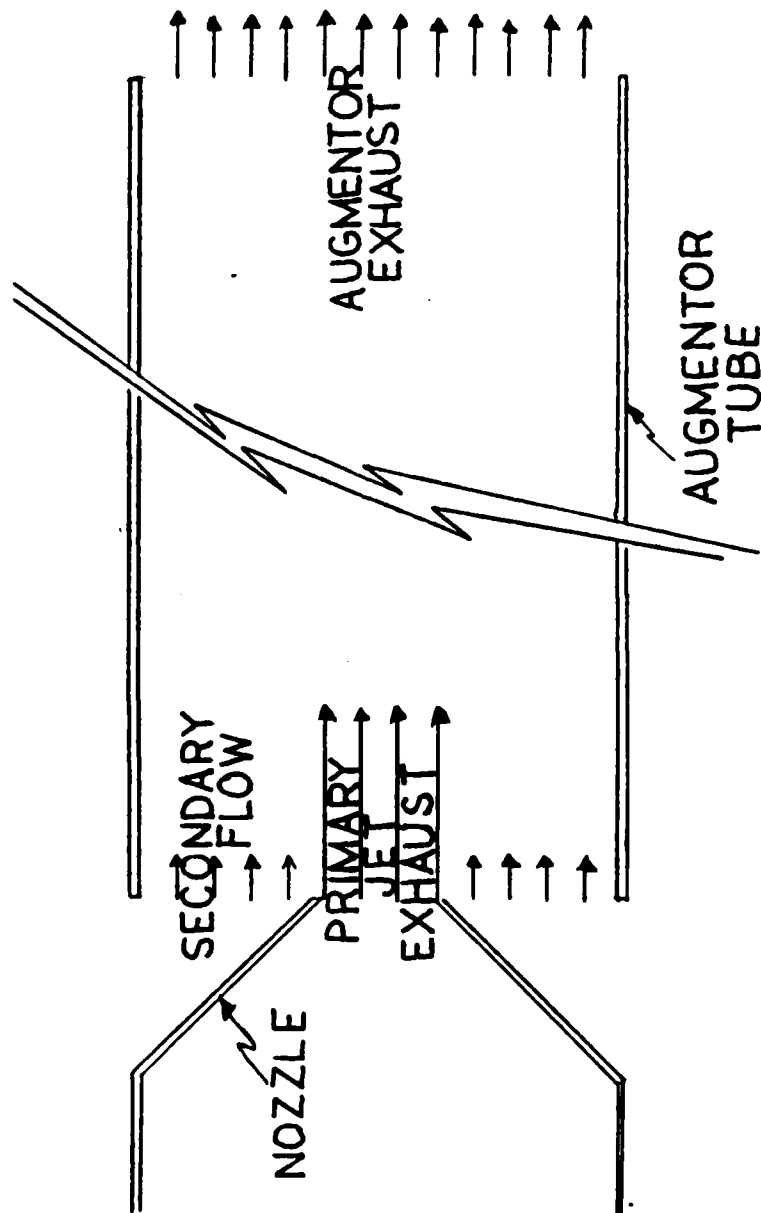


Figure 5. Augmentor Tube Flow

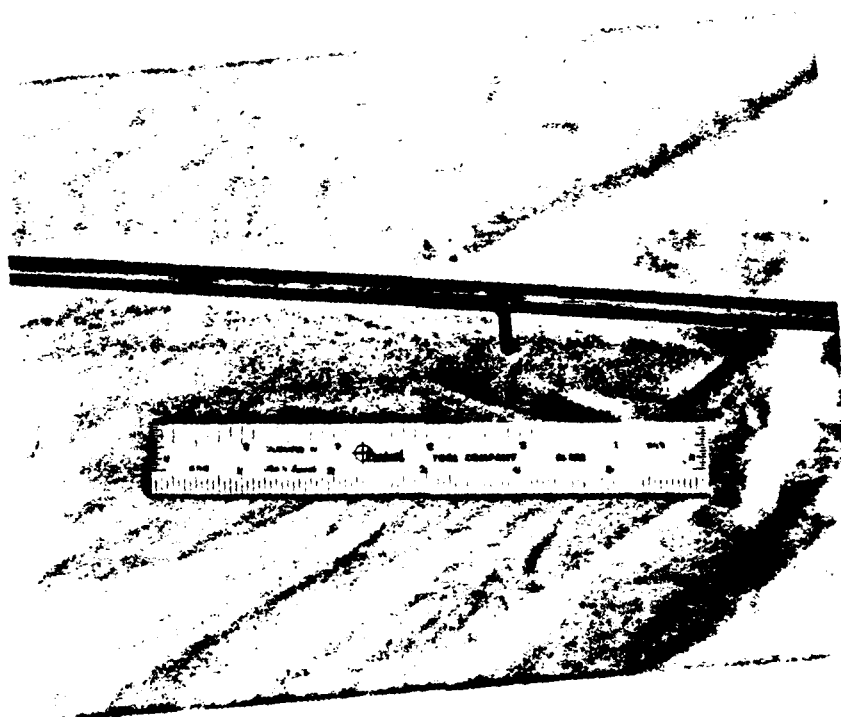


Figure 6. Traversing Kiel Probe

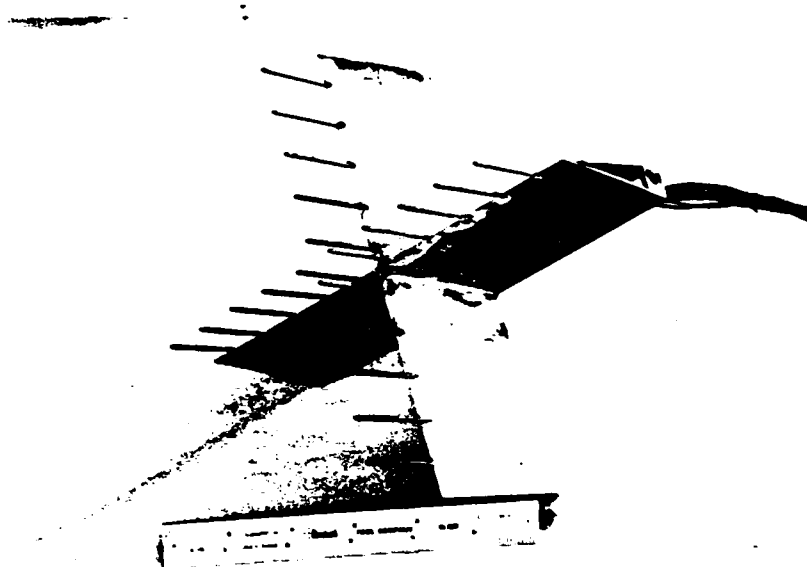


Figure 7. Stationary Pitot Rake

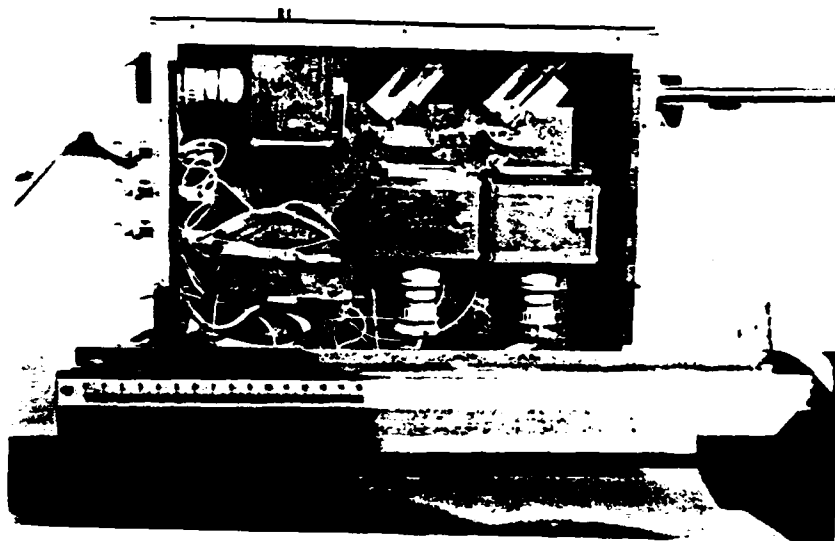


Figure 8. Three Wavelength Light Transmission Box

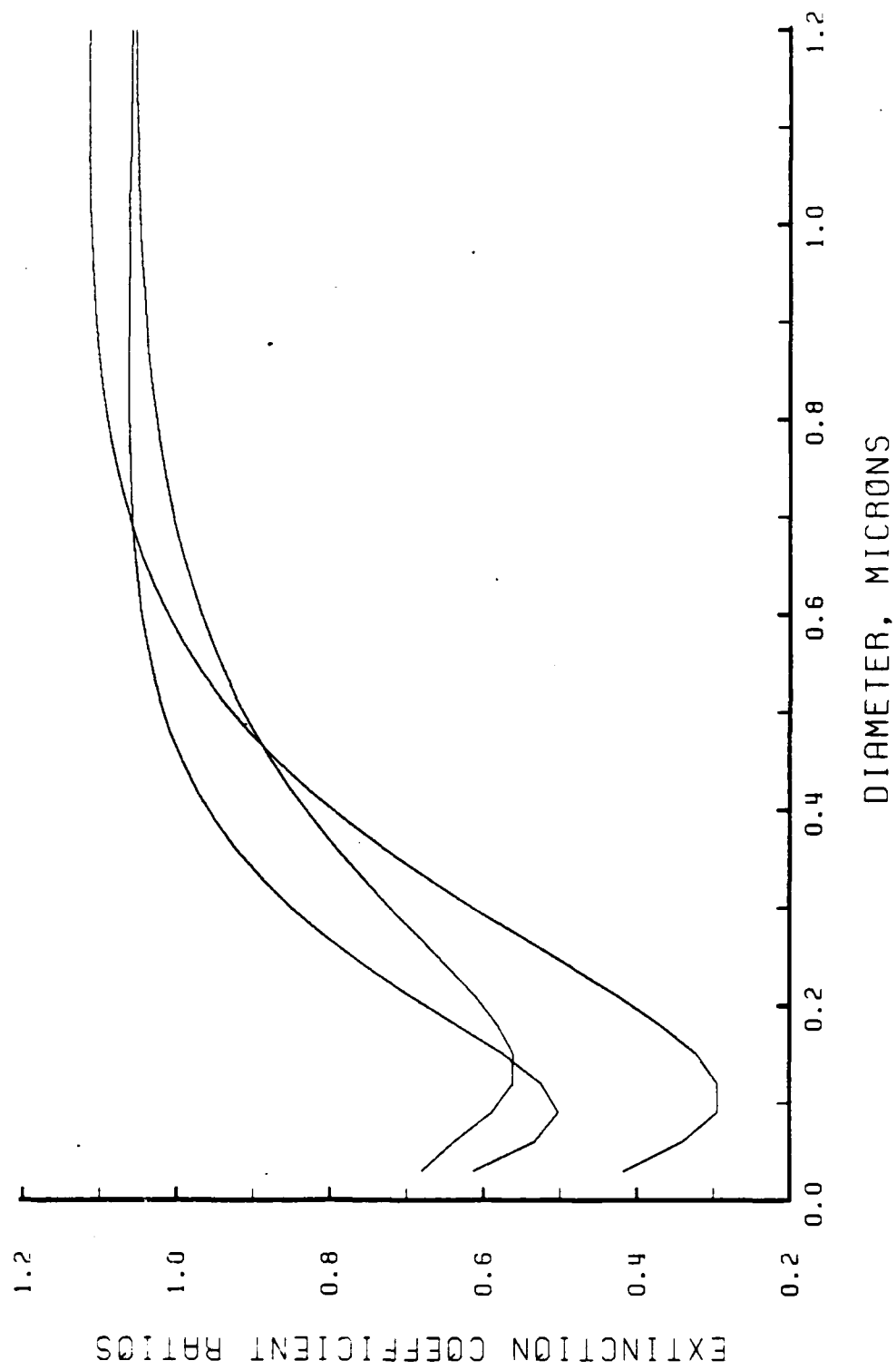
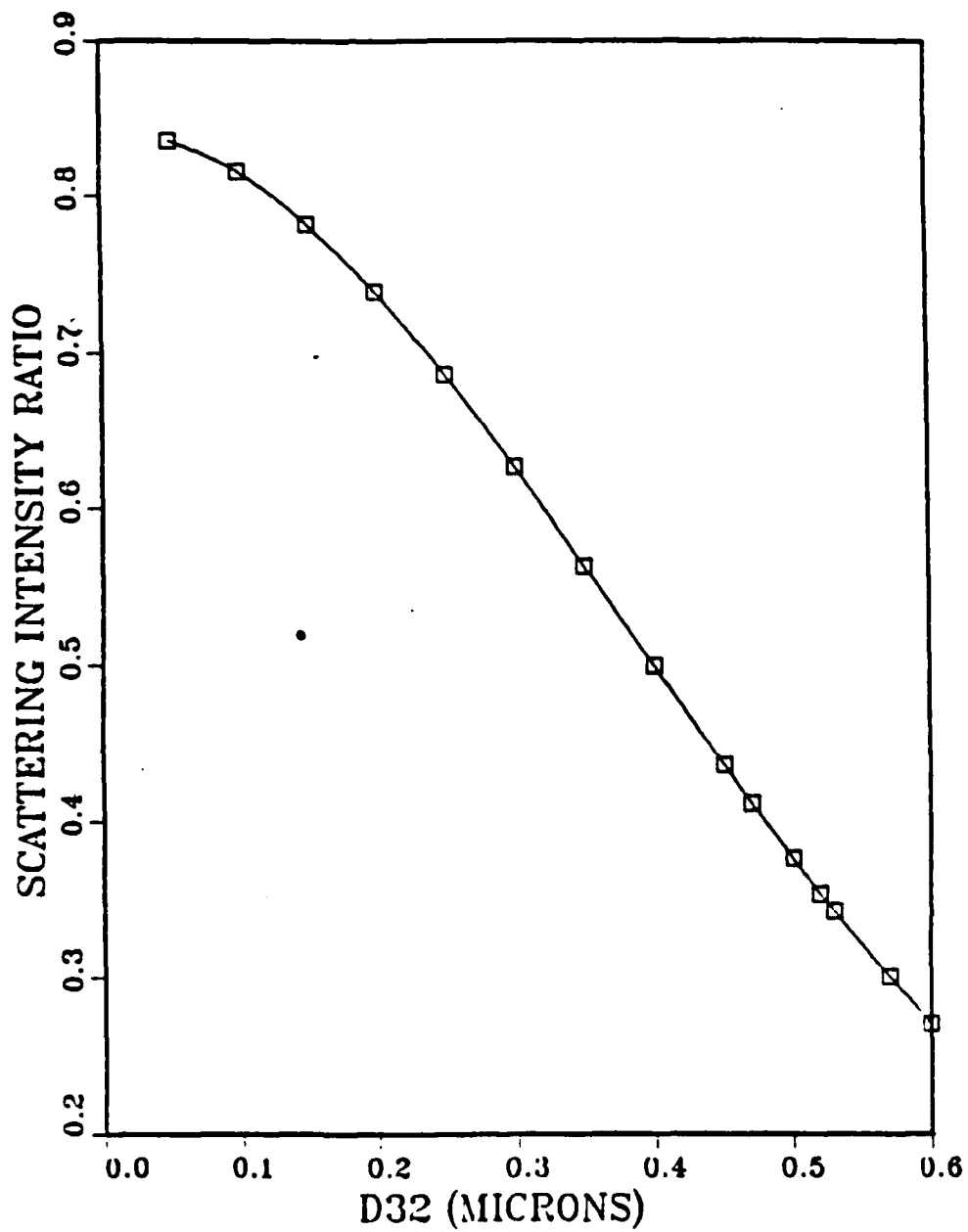


Figure 9. Extinction Coefficient Ratio versus Particle Diameter



Scattered Light Intensity Ratio  
(40°/20°) vs. Particle Size (d32)  
for .6328 Micron Wavelength Light

Figure 10. Light Intensity Ratio versus Particle Diameter

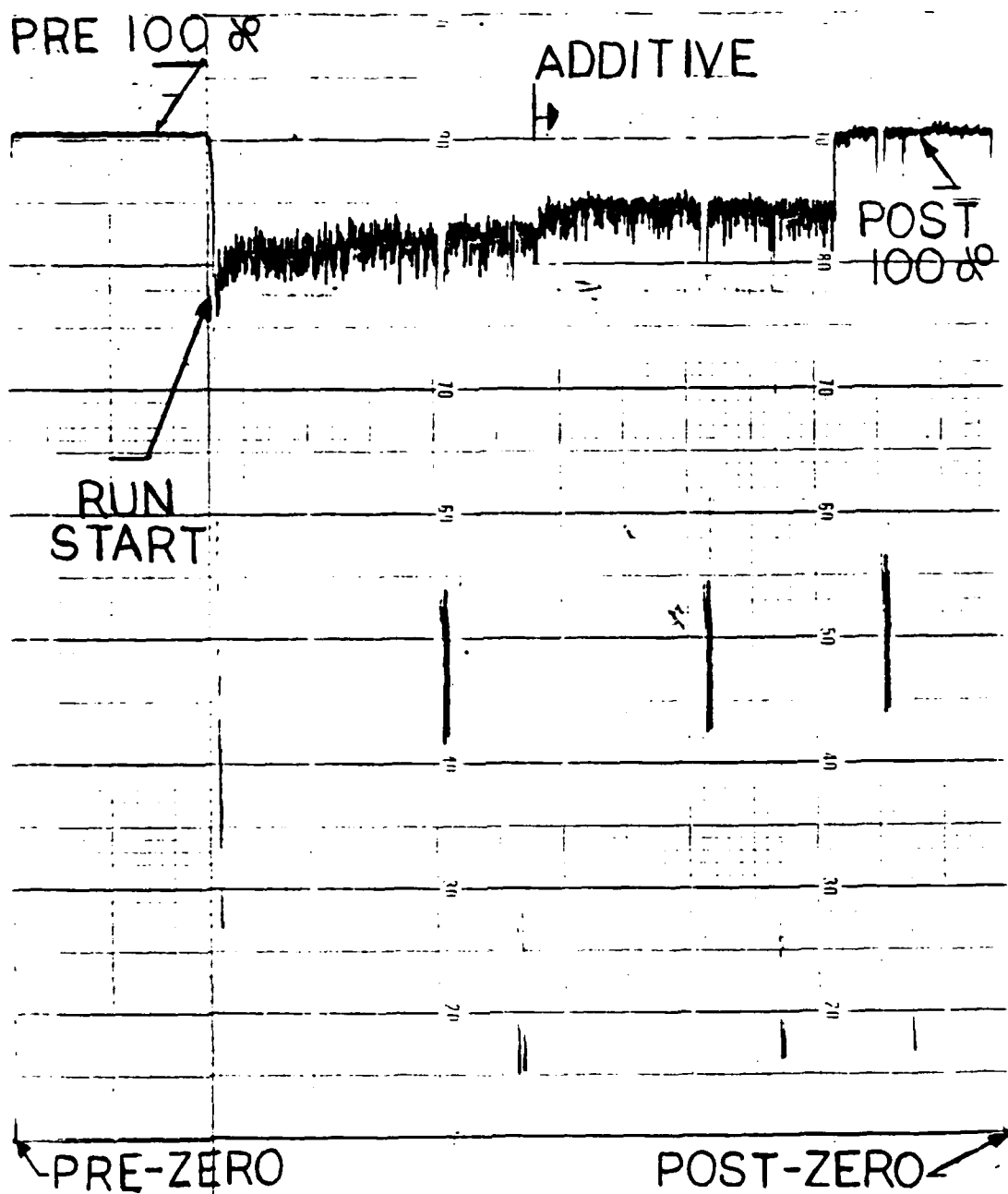


Figure 11. Sample Transmittance Data from Stripchart

# VELOCITY PROFILES (RUN #1)

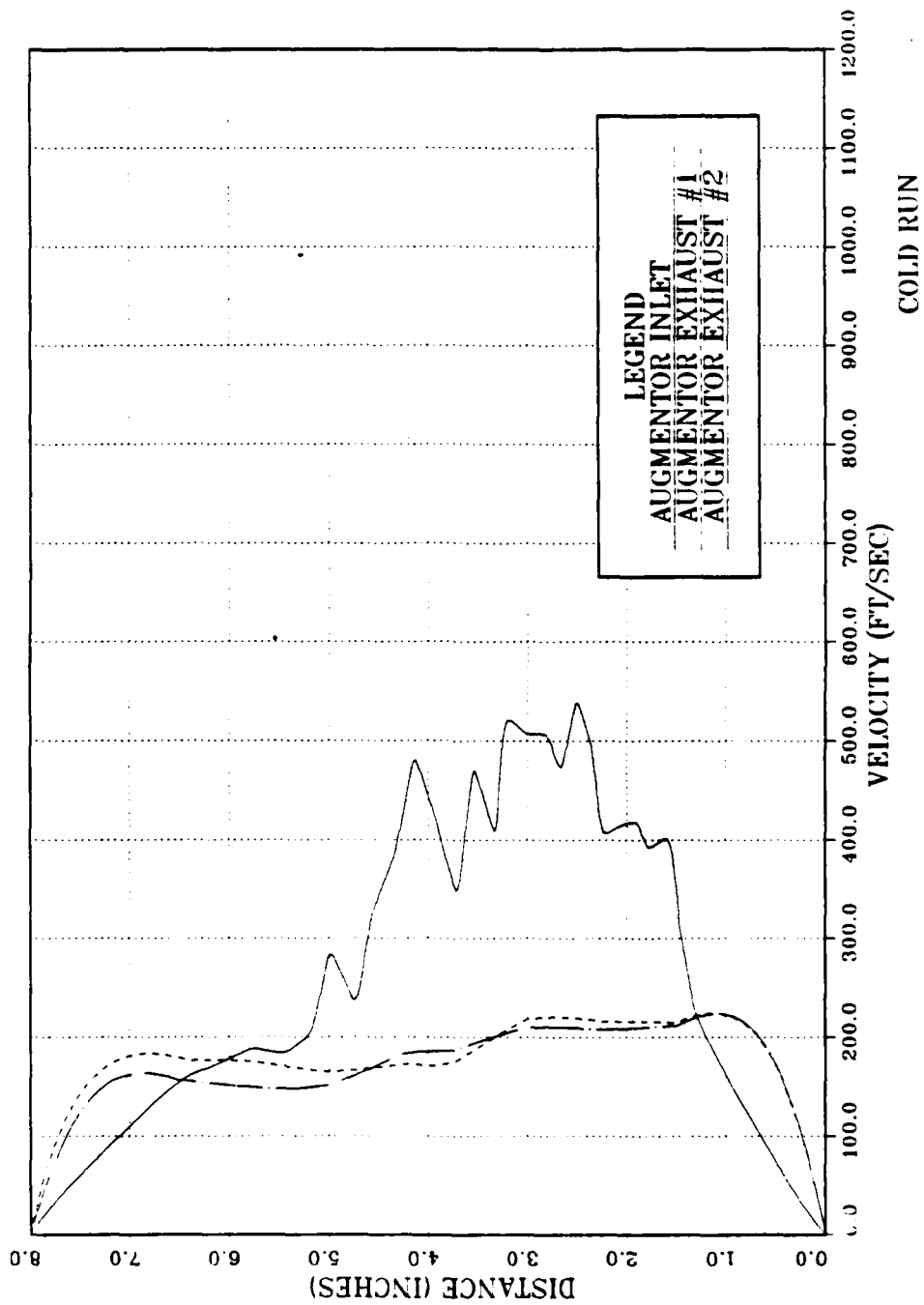


Figure 12. Velocity versus Radial Distance Graph  
 $s = 12$  in,  $AR = 3.5$

# VELOCITY PROFILES (RUN#2)

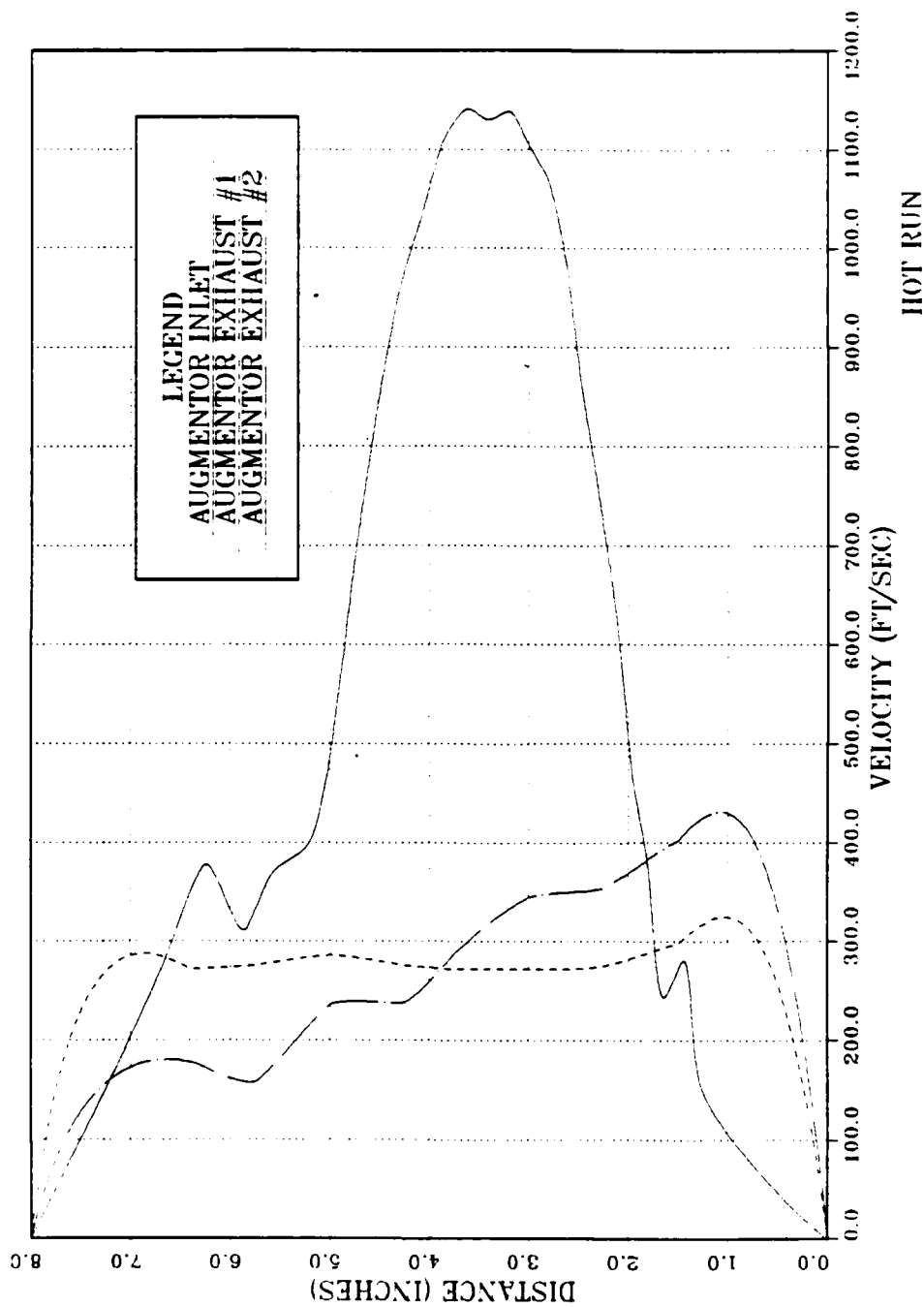


Figure 13. Velocity versus Radial Distance Graph,  $s = 12$  in,  $AR = 3.8$

# VELOCITY PROFILES (RUN#3)

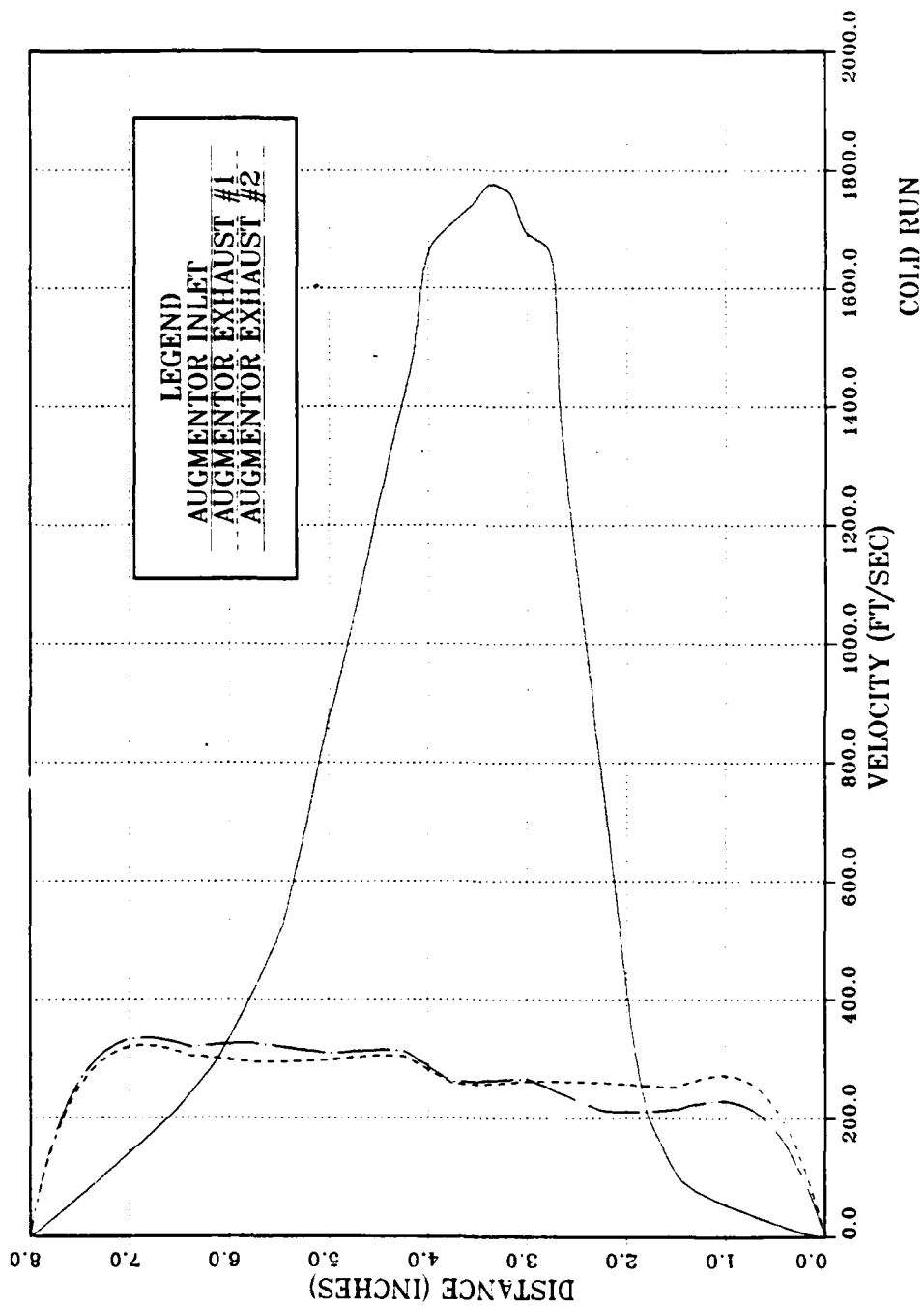


Figure 14. Velocity versus Radial Distance Graph,  $s = 3\text{in}$ ,  $AR = 5.2$

# PARTICLE SIZE VS FUEL-AIR RATIO

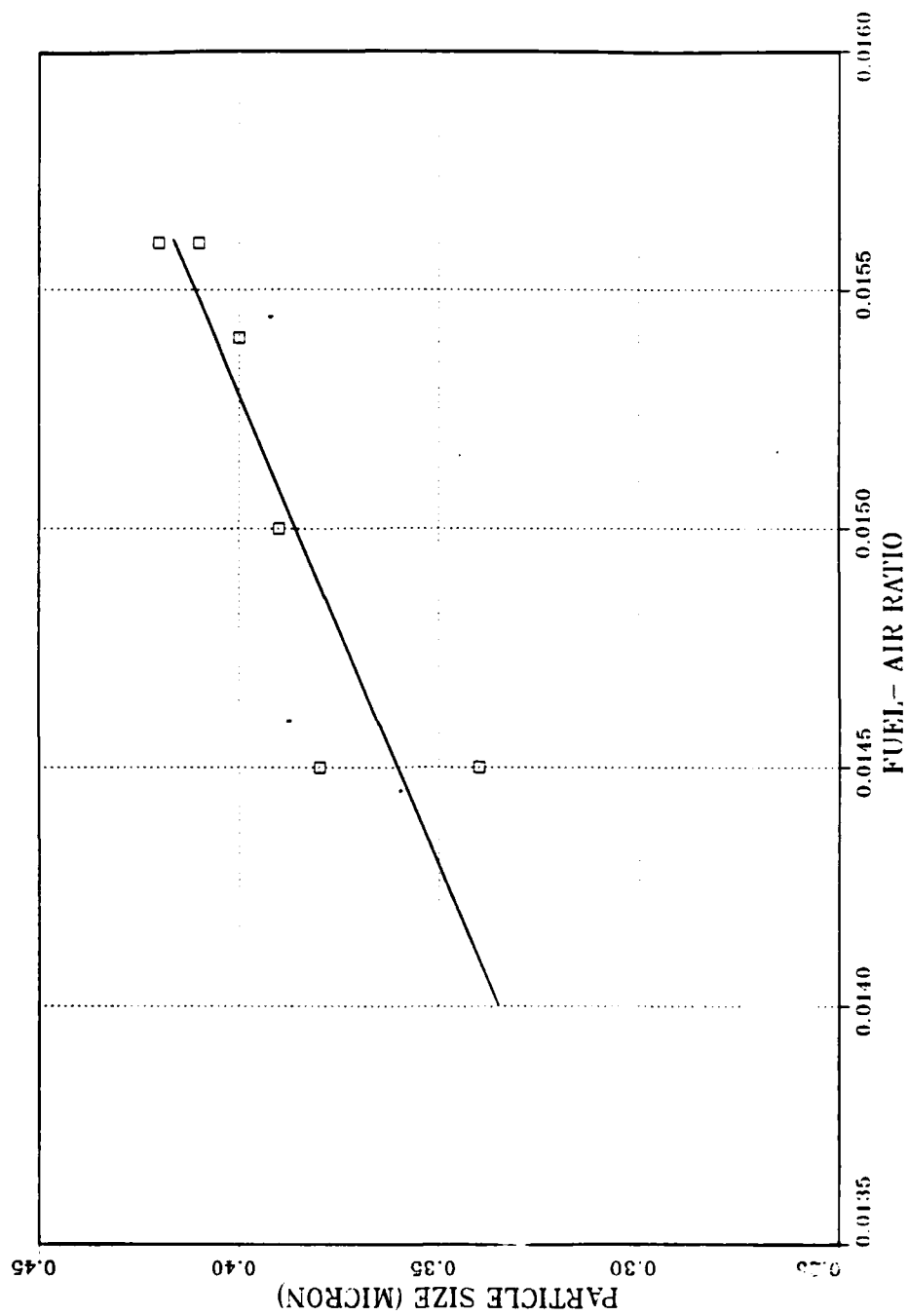


Figure 15. Particle Size versus Fuel-Air-Ratio

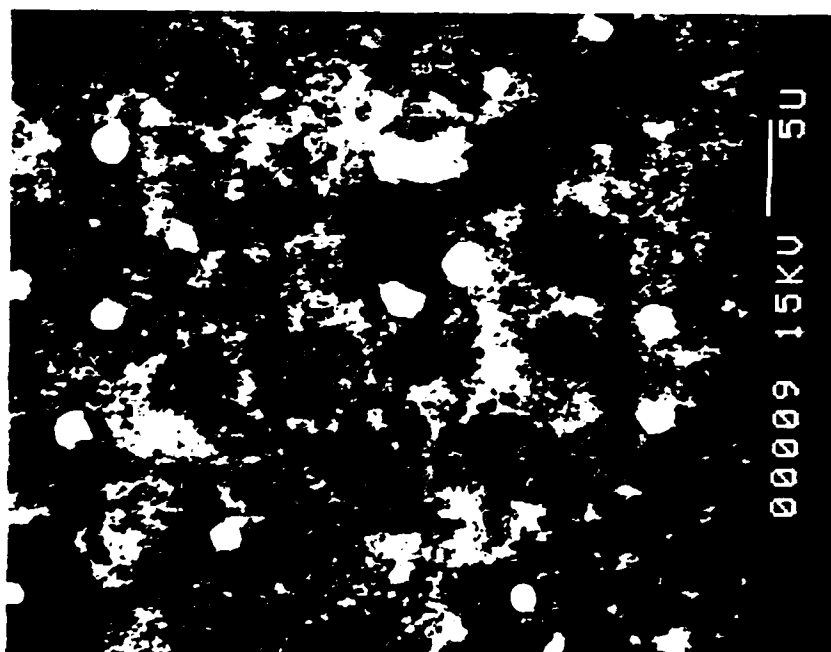
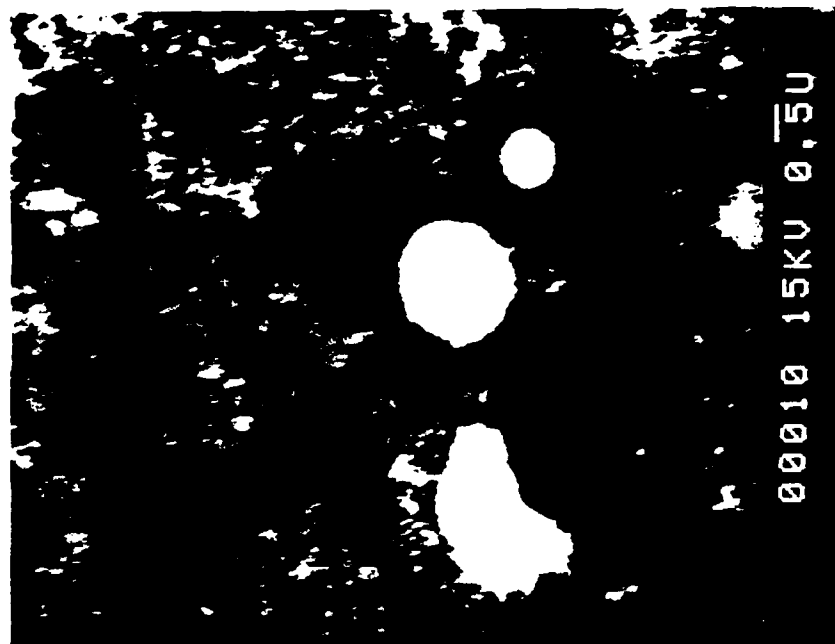
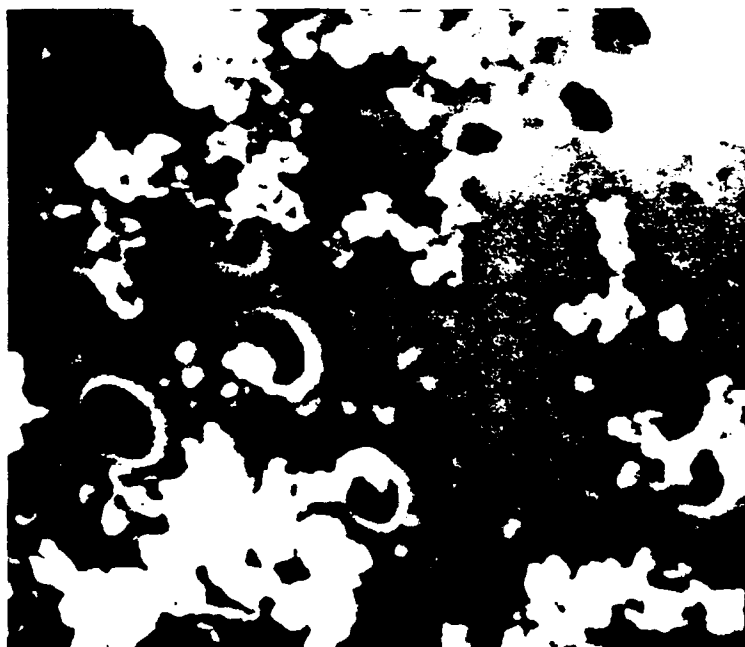
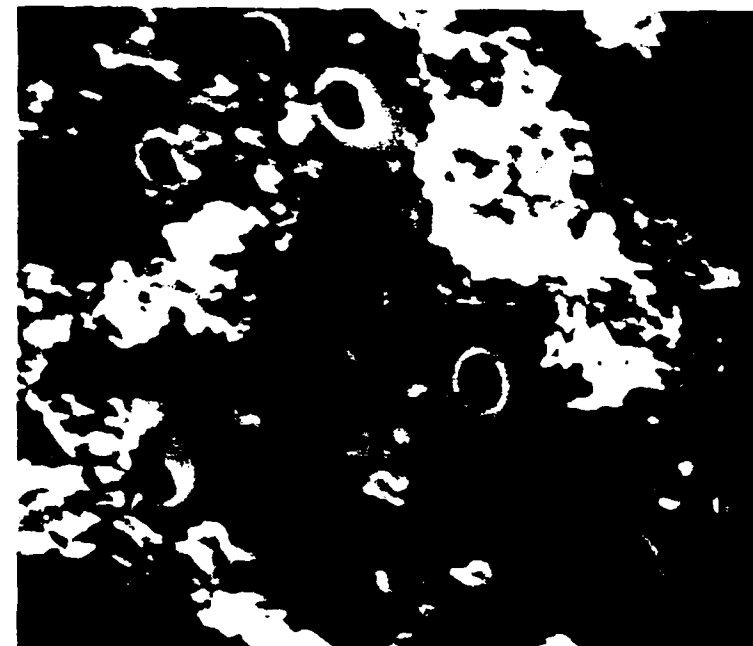


Figure 16. Scanning Electron Microscope Photograph,  
Impact Sample



00007 15KV 0.5U

Figure 17. Scanning Electron Microscope Photograph,  
Filtered Sample

## APPENDIX B

TABLES

TABLE 1  
TRAVERSING PROBE VELOCITY AND TEMPERATURE DATA RUN #1

Probe Station Number	Distance from Augmentor Wall Inches	Total Pressure Psig	Static Pressure Psig	Total Temperature °R	Velocity ft/sec	Mach Number	Temperature °R
1	0	0	0	523	0	0	523
2	1.32	.433	-.029	510	231	.21	505
3	1.47	.832	-.055	508	317	.29	499
4	1.62	1.430	-.042	505	402	.37	492
5	1.77	1.364	-.029	505	392	.36	492
6	1.91	1.563	-.042	503	418	.39	489
7	2.05	1.563	-.029	501	416	.38	487
8	2.20	1.497	-.022	501	406	.37	488
9	2.35	2.228	-.055	501	491	.46	481
10	2.50	2.760	-.042	502	539	.50	478
11	2.67	2.029	-.067	502	473	.44	484
12	2.83	2.428	-.022	503	508	.47	481
13	3.00	2.428	-.016	503	507	.47	482
14	3.17	2.561	-.029	504	521	.48	482
15	3.34	1.497	-.035	504	409	.38	490
16	3.53	2.029	-.029	505	469	.43	486
17	3.72	1.031	-.055	505	348	.32	495
18	3.93	1.563	-.055	506	421	.39	490
19	4.13	2.095	-.061	506	481	.44	487
20	4.34	1.297	-.048	507	386	.35	495
21	4.56	.898	-.048	508	327	.30	500
22	4.75	.437	-.055	510	237	.22	505
23	4.98	.632	-.074	510	285	.26	504
24	5.21	.300	-.048	512	202	.18	509
25	5.46	.233	-.055	514	184	.17	511
26	5.77	.300	-.003	516	188	.17	512
27	6.07	-	-.048	517	-	-	-
28	6.38	.167	-.055	518	162	.15	516
29	8.00	0	0	523	0	0	523

TABLE 2

## X-RAKE VELOCITY AND RUN DATA, RUN #1

Rake Probe Number	Total Pressure Psig	Velocity ft/sec	Mach Number	Mass Flow Section Lbm/sec	Temp °R
1	.615	208	.19	.525	507
2	.640	215	.19	.421	507
3	.645	216	.20	.303	507
4	.659	219	.20	.184	507
5	.504	175	.16	.049	509
6	.497	173	.16	.048	509
7	.475	165	.15	.139	509
8	.504	175	.16	.245	509
9	.508	176	.16	.345	508
10	.487	169	.15	.426	509
11	.620	209	.19	.528	507
12	.628	212	.19	.415	507
13	.614	208	.19	.291	507
14	.622	210	.19	.176	507
15	.542	187	.17	.052	508
16	.530	183	.17	.051	508
17	.438	152	.14	.127	509
18	.431	149	.14	.209	509
19	.450	156	.14	.306	509
20	.436	151	.14	.380	509

Mass Flow Primary = 1.16 Lbm/sec

Mass Flow Secondary = 3.59 Lbm/sec

Total Mass Flow = 5.22 Lbm/sec

Augmentation Ratio = 3.51

 $P_{\text{static}} = .239$  Psig $P_{\text{atmos}} = 14.9$  psi $T_t = 511$  °RNozzle to Augmentor = 12 inches  
Spacing

TABLE 3  
TRAVERSING PROBE VELOCITY AND TEMPERATURE DATA, RUN #2

Probe Station Number	Distance From Augmentor Wall Inches	Total Pressure Psig	Static Pressure Psig	Total Temperature °R	Velocity ft/sec	Mach Number	Temperature °R
1	0	0	0	522	0	0	522
2	1.29	0	-.210	526	161	.14	524
3	1.46	.469	-.175	528	279	.25	521
4	1.62	.235	-.253	530	245	.22	525
5	1.80	.938	-.218	535	374	.33	523
6	1.95	1.563	-.227	541	462	.41	523
7	2.12	3.204	-.244	548	625	.56	516
8	2.29	4.924	-.210	556	745	.67	510
9	2.47	7.112	-.218	562	864	.79	500
10	2.64	10.473	-.227	565	997	.92	482
11	2.82	13.755	.131	564	1073	1.01	468
12	3.01	16.491	.768	561	1107	1.05	459
13	3.20	18.445	.934	558	1139	1.09	450
14	3.41	18.132	.969	557	1130	1.08	451
15	3.61	16.882	.026	553	1142	1.10	445
16	3.83	15.553	-.131	550	1116	1.08	446
17	4.06	12.349	-.297	547	1041	.99	457
18	4.28	9.848	-.410	543	968	.91	466
19	4.53	6.643	-.375	541	837	.78	482
20	4.77	3.751	-.384	539	673	.61	501
21	4.99	1.798	-.279	536	493	.44	516
22	5.26	1.016	-.277	533	393	.35	520
23	5.55	0.860	-.297	528	372	.33	517
24	5.87	0.547	-.253	526	311	.28	518
25	6.23	0.938	-.271	523	378	.34	511
26	6.60	0.860	-	523	296	.27	515
27	8.00	0	0	522	0	0	522

TABLE 4

## X-RAKE VELOCITY AND RUN DATA, RUN #2

Rake Probe Number	Total Pressure Psig	Velocity Ft/sec	Mach Number	Mass Flow Section Lbm/sec	Temp °R
1	1.222	308	.28	.777	498
2	1.170	298	.27	.587	498
3	1.048	275	.25	.386	499
4	1.033	272	.25	.229	499
5	1.034	273	.25	.076	499
6	1.051	276	.25	.078	499
7	1.103	286	.26	.241	499
8	1.051	276	.25	.387	499
9	1.033	272	.25	.536	499
10	1.020	270	.25	.681	500
11	1.874	403	.37	1.019	492
12	1.862	402	.37	.791	492
13	1.512	354	.32	.497	495
14	1.451	345	.32	.291	496
15	1.114	288	.26	.081	499
16	.873	238	.22	.067	501
17	.868	237	.21	.199	501
18	.589	158	.14	.222	504
19	.649	178	.16	.350	503
20	.588	157	.14	.397	504

Mass Flow Primary = 1.63 Lbm/sec

Mass Flow Secondary = 6.26

Total Mass Flow = 7.89

Augmentation Ratio = 3.84

 $P_{\text{static}} = .371$  $P_{\text{atmos}} = 14.7$  $T_t = 506 \text{ } ^\circ\text{R}$ 

Nozzle to Augmentor Spacing

TABLE 5

## TRAVERSING PROBE VELOCITY AND TEMPERATURE DATA, RUN #3

Probe Station Number	Distance from Augmentor Wall Inches	Total Pressure Psig	Static Pressure Psig	Total Temperature °R	Velocity ft/sec	Mach Number	Temperature °r
1	0	0	0	524	0	0	524
2	1.48	.053	-.026	568	102	.09	565
3	1.63	.112	-.045	601	148	.12	600
4	1.78	.288	.006	630	202	.16	627
5	1.92	.640	-.006	696	319	.25	688
6	2.07	1.404	-.168	790	522	.39	767
7	2.21	2.696	-.155	884	725	.51	840
8	2.36	4.164	-.161	1002	926	.62	930
9	2.53	6.631	-.155	1098	1164	.76	983
10	2.68	9.743	-.155	1219	1413	.90	1049
11	2.85	12.797	-.155	1425	1678	1.00	1188
12	3.01	15.205	.683	1400	1694	1.03	1154
13	3.19	16.380	.670	1443	1765	1.06	1176
14	3.37	16.615	.638	1447	1778	1.07	1177
15	3.55	16.027	.657	1425	1742	1.05	1163
16	3.74	14.794	.090	1384	1714	1.05	1133
17	3.96	13.150	-.071	1410	1677	1.01	1171
18	4.16	11.035	-.058	1235	1478	.94	1049
19	4.38	9.039	-.064	1148	1329	.86	1000
20	4.59	6.866	-.200	1061	1164	.78	946
21	4.79	5.456	-.193	973	1020	.70	885
22	5.03	3.812	-.187	906	852	.60	845
23	5.26	2.402	-.193	825	673	.49	787
24	5.49	1.404	-.187	756	514	.39	733
25	5.80	.816	-.200	697	399	.31	683
26	6.15	.405	-.187	627	292	.24	620
27	6.48	.170	-.200	586	224	.19	582
28	0	0	0	524	0	0	524

TABLE 6

RUN 3 x RAKE (HOT RUN)

Rake Probe Number	Total Pressure Psig	Velocity Ft/sec	Mach Number	Mass Flow Section Lbm/sec	Temp °R
1	.791	258	.20	.468	703
2	.770	252	.19	.356	703
3	.796	259	.20	.262	703
4	.802	261	.20	.158	703
5	.791	258	.20	.052	703
6	.956	303	.24	.061	701
7	.934	297	.23	.180	701
8	.919	294	.23	.296	701
9	.962	305	.24	.431	701
10	.944	300	.23	.545	701
11	.659	215	.17	.390	705
12	.659	214	.17	.303	705
13	.654	213	.16	.215	705
14	.814	265	.21	.160	703
15	.799	260	.20	.052	703
16	.994	312	.24	.063	700
17	.980	309	.24	.187	701
18	1.047	325	.25	.328	700
19	1.023	319	.25	.452	700
20	.989	311	.24	.565	701

Mass Flow Primary = .892

Mass Flow Secondary = 4.637

Total Mass Flow = 5.529

Augmentation Ratio = 5.199

 $P_{\text{static}} = .368$  $P_{\text{atmos}} = 14.8$  $T_T = 708 \text{ } ^\circ\text{R}$ Nozzle to Augmentor = 3 inches  
Spacing

TABLE 7

## SUMMARY OF OPTICAL DATA

Run Number	Additive	Transmittances		3 Wavelength D <sub>32</sub> (microns)			Intensity Ratio I <sub>40</sub> /I <sub>20</sub>	Scattering D <sub>32</sub> (microns)
		T <sub>100</sub>	T <sub>694.3</sub>	T <sub>450</sub>	1000 694.3	694.3 450	1000 450	
2		.952	.944	.943	.43	.41	.42	-
6		.851	.848	.844	.65	.42	.52	-
7a	Ferrocene	.926	.923	.923	.6	.47	.54	-
8		.862	.860	.863	.64	.48	.57	.34
8a	12% Cerium	.934	.905	.901	.27	.38	.33	.38
9		.784	.854	.850	*	.42	*	.40
9a	12% Cerium	.891	.896	.893	*	.42	*	.43
10		.862	.862	.861	*	.47	*	.39
10a	12% Cerium	.925	.926	.926	*	.47	*	.41
11		.885	.887	.883	*	.40	*	.42
11a	USIAD-2055	.907	.913	.913	*	.47	*	.43
12		.907	.911	.913	*	.50	*	.41
12a	USIAD-2055	.908	.898	.893	.46	.38	.43	.43
13		.924	.963	.923	*	*	*	.31
13a	12% Cerium	-	-	-	-	-	-	.42
14		.918	.894	.891	.33	.41	.37	.38
14a	12% Cerium	.919	.923	.896	*	.38	*	.41

Fuel = NAPC #7 Augmentor to Nozzle Spacing = Flush Blanking Plate Installed  
 Augmentation Ratio = .53

- = Not Collected

\* = No Correlation

a = additive run

TABLE 8  
PHYSICAL AND CHEMICAL PROPERTIES OF NAPC FUEL #7

API Gravity @ 15°C -----	35.6
Distillation (ASTM) IBP deg. C -----	193
Composition Aromatics (vol %) max. ---	26.4
Olefins (vol %) max. -----	.86
Hydrogen Content, (wt %), min. -----	12.83
Smoke Point, min. -----	14.0
Aniline-Gravity Prod., min. -----	4,254
Freeze Point, deg. C -----	-31.0
Viscosity @ 37.8 deg. C (cSt) -----	1.77
Temperature @ 12 cSt, deg. C -----	-30.6

TABLE 9

## SUMMARY OF PARTICLE SIZE

Run Number	Fuel Flow Gal/min	Temperature T <sub>engine exhaust</sub>	T <sub>augmentor exhaust</sub>	Additive	D <sub>32</sub> Engine Exhaust	D <sub>32</sub> Augmentor Transmittance	D <sub>32</sub> Augmentor Scattering
2	.0156	1630	1157	None	.18-.21	.41-.43	-
6	.0150	1630	1157	None	.19-.22	.42-.65	-
7a	.0153	1642	1131	Ferrocene	.17-.23	.47-.60	-
8	.0145	1594	1136	None	.18-.25	.48-.64	.34
8a	.0143	1580	1136	12% Cerium Hex	.19-.23	.27-.38	.38
9	.0154	1635	1130	None	.18-.20	* .42 *	.40
9a	.0152	1641	-	12% Cerium Hex	.19-.20	* .42 *	.43
10	.0150	1632	1121	None	.17-.22	* .47 *	.39
10a	.0149	1640	-	12% Cerium Hex	.18-.20	* .47 *	.41
11	.0156	1664	1179	None	-	* .40 *	.42
11a	.0156	1690	-	USLAD-2055	-	* .47 *	.43
12	.0156	1632	1128	None	-	* .50 *	.41
12a	.0154	1628	-	USLAD-2055	-	.38-.46	.43
13	.0142	1764	1235	None	.15-.18	-	.31
13a	.0141	1760	-	12% Cerium Hex	-	-	.42
14	.0145	1643	1088	None	.26 (scat)	.33-.41	.38
14a	.0145	1684	-	12% Cerium Hex	.17 (scat)	* .38 *	.41

Fuel NAPC #7      Augmentation Ratio = .53      Augmentor Blocking Plate Installed

Scat = Engine Exhaust Scattering Technique      \* = No Correlation      - = Not Collected

#### LIST OF REFERENCES

1. Krug, A.C., An Experimental Investigation of Soot Behavior in a Gas Turbine Combustor, M.S. Thesis, Naval Postgraduate School, Monterey, California, June 1983.
2. Dubeau, R.W., A Gas Turbine Combustor Test Facility for Fuel Composition Investigation, M.S. Thesis, Naval Postgraduate School, Monterey, California, June 1983.
3. Lohman, A.L., An Investigation into the Soot Production Process in a Gas Turbine Engine, M.S. Thesis, Naval Postgraduate School, Monterey, California, September 1984.
4. Bennett, J.S., An Investigation of Particular Size Measurement Using Non-intrusive Optical Techniques in a Gas Turbine Engine, M.S. Thesis, Naval Postgraduate School, Monterey, California, September 1985.
5. Naval Postgraduate School Report No. NPS67-80-014, Validation of a Two-dimensional Primitive Variable Computer Code for Flow Field in Jet Engine Test Cells, by P.J. Mallon, P.J. Hickey, D.W. Netzer, October 1980.
6. Naval Postgraduate School Report No. NPS67-82-13, An Investigation of the Effectiveness of Smoke Suppressant Fuel Additives for Turbojet Applications, by J.R. Bramer, D.W. Netzer, September 1982.
7. Naval Postgraduate School Report No. NPS67-81-001, Temperature Dependence of Gas Properties in Polynomial Form, by J.R. Andrews, O. Biblarz, January 1981.
8. Cashdollar, K.L., Lee, C.K., and Singer, J.M., "Three-Wavelength Light Transmission Technique to Measure Smoke Particle Size and Concentration," Applied Optics, Volume 18, Number 11, June 1979.
9. Powell, E.A. and others, Combustion Generated Smoke Diagnostics by Means of Optical Techniques, American Institute of Aeronautics and Astronautics, 14th Aerospace Sciences Meeting, January 1976, AIAA paper Number 76-67.

INITIAL DISTRIBUTION LIST

	No. Copies
1. Defense Technical Information Center Cameron Station Alexandria, Virginia 22304-6145	2
2. Library, Code 0142 Naval Postgraduate School Monterey, California 93943-5000	2
3. Department Chairman, Code 67 Department of Aeronautics Naval Postgraduate School Monterey, California 93943-5000	1
4. Professor D.W. Netzer, Code 67Nt Department of Aeronautics Naval Postgraduate School Monterey, California 93943-5000	2
5. Professor D. Salinas Department of Mechanical Engineering Naval Postgraduate School Monterey, California 93943-5000	1
6. LT. Dave Jeffrey Urioh Naval Air Rework Facility Naval Air Station Alameda Alameda, California 94501	2

END

11-86

DTIC